Behavioral/Cognitive

Causal Control of Medial–Frontal Cortex Governs Electrophysiological and Behavioral Indices of Performance Monitoring and Learning

Robert M. G. Reinhart and Geoffrey F. Woodman

Department of Psychology, Center for Integrative and Cognitive Neuroscience, Vanderbilt Vision Research Center, Vanderbilt University, Nashville, Tennessee 37240

Adaptive human behavior depends on the capacity to adjust cognitive processing after an error. Here we show that transcranial direct current stimulation of medial–frontal cortex provides causal control over the electrophysiological responses of the human brain to errors and feedback. Using one direction of current flow, we eliminated performance-monitoring activity, reduced behavioral adjustments after an error, and slowed learning. By reversing the current flow in the same subjects, we enhanced performance-monitoring activity, increased behavioral adjustments after an error, and sped learning. These beneficial effects fundamentally improved cognition for nearly 5 h after 20 min of noninvasive stimulation. The stimulation selectively influenced the potentials indexing error and feedback processing without changing potentials indexing mechanisms of perceptual or response processing. Our findings demonstrate that the functioning of mechanisms of cognitive control and learning can be up- or down-regulated using noninvasive stimulation of medial–frontal cortex in the human brain.

Key words: **executive control; learning; medial–frontal cortex; transcranial direct current stimulation**

Introduction

Event-related potential (ERP) and neuroimaging studies have shaped our view of how executive mechanisms monitor our behavior and respond to errors so we can improve information processing (Ridderinkhof et al., 2004; Brown and Braver, 2005; Gehring et al., 2012; Sheth et al., 2012; Zhua et al., 2012). This research has identified two medial–frontal potentials indexing the monitoring of task performance. The error-related negativity (ERN) and the feedback-related negativity (FRN) are observed shortly after an errant behavioral response (Falkenstein et al., 1990; Gehring et al., 1993) and negative feedback (Miltner et al., 1997), respectively. These potentials are hypothesized to be generated in the medial–frontal lobe (particularly the anterior cingulate cortex) by executive control mechanisms that detect errors (Falkenstein et al., 1990; Gehring et al., 1993, 2012; Miltner et al., 1997) or more generally support learning (Holroyd and Coles, 2002; Brown and Braver, 2005; Alexander and Brown, 2011). Our goal here was to test these hypotheses using causal manipulations of medial–frontal cortex. In addition, we used a type of electrical stimulation that can increase activity in an area, resulting in the prediction that, if these hypotheses are correct, then we should be able to improve executive control and learning.

We causally manipulated medial–frontal cortex using transcranial direct current stimulation (tDCS) (Utz et al., 2010) while recording subjects' ERN and FRN to assess the efficacy of our stimulation in affecting the mechanisms of interest. We noninvasively passed current through medial–frontal cortex (i.e., the anterior cingulate cortex [ACC] and supplementary motor area [SMA]; for details of the current flow model, see Fig. 1*A* and Fig. 10) (Dehaene et al., 1994; Carter et al., 1998). Anodal stimulation has been shown to up-regulate neural activity in a targeted region, whereas cathodal stimulation down-regulates neural activity (Bindman et al., 1962; Nitsche and Paulus, 2001; Nitsche et al., 2003c), depending on certain stimulation parameters, such as intensity level and duration (Batsikadze et al., 2013; Monte-Silva et al., 2013). This gave us bidirectional causal control over activity in medial–frontal cortex.

First, we predicted that manipulating medial–frontal cortex and the electrophysiological signatures of performance monitoring (i.e., the ERN and FRN) should allow us to influence subjects' detection and reactions to errors (Falkenstein et al., 1990; Gehring et al., 1993; Miltner et al., 1997), resulting in changes in error rates as well as the speed and accuracy of responses after the commission of an error. Second, we tested the hypothesis that medial–frontal activity underlies our ability to rapidly learn new tasks (Holroyd and Coles, 2002; Brown and Braver, 2005; Alexander and Brown, 2011). In a previous study, repetitive transcranial magnetic stimulation over medial–frontal cortex reduced ERN amplitude and posterror behavioral accuracy (Rollnik et al.,

Received Dec. 28, 2013; revised Jan. 23, 2014; accepted Jan. 30, 2014.

Author contributions: R.M.G.R. and G.F.W. designed research; R.M.G.R. performed research; R.M.G.R. analyzed data; R.M.G.R. and G.F.W. wrote the paper.

This work was supported by National Institutes of Health Grants R01-EY019882, P30-EY08126, and P30-HD015052 and National Science Foundation Grant BCS-0957072.

The authors declare no competing financial interests.

Correspondence should be addressed to Dr. Geoffrey F. Woodman, PMB 407817, 2301 Vanderbilt Place, Vanderbilt University, Nashville, TN 37240-7817. E-mail: geoffrey.f.woodman@vanderbilt.edu.

DOI:10.1523/JNEUROSCI.5421-13.2014

 0270-6474/14/344214-14$15.00/0

2004). The advance of the current study is to test multiple hypotheses about the functional significance of medial–frontal cortex and its electrophysiological indices. Further, we sought to determine whether we could exert bidirectional control over medial–frontal activity and potentially enhance the medial–frontal ERPs and the high-level cognitive functions they index.

Materials and Methods

Subjects. Subjects gave informed consent before procedures approved by the Vanderbilt University Institutional Review Board and were provided financial compensation. We conducted four experiments with each using a within-subjects design: the principal 3 day experiment (Experiment 1, $N = 18$, mean ± SD age 26 ± 5.2, 10 female), a 2 day experiment examining the duration of the primary beneficial effects observed in Experiment 1 (Experiment 2, $N = 18$, mean ± SD age 22 ± 3.7, 4 female), a 3 day experiment controlling for the reference electrode location (Experiment 3, $N = 10$, mean ± SD age 24 ± 3.4, 6 female), and a 3 day experiment extending our findings to a simpler paradigm (Experiment 4, $N = 18$, mean ± SD age 22 ± 4.5, 8 female). All subjects reported no history of neurological problems, such as seizures, multiple sclerosis, or head trauma. All subjects reported to be right-handed, have normal color vision, and normal or corrected-to-normal visual acuity.

The necessary sample size was estimated from a pilot experiment using a sample of 10 subjects, all of whom received sham, anodal, and cathodal tDCS on 3 separate days. By conservatively pooling mean difference and SD values in behavioral and electrophysiological responses between active and sham tDCS conditions, we estimated Cohen's *d* effect size based on paired samples two-tailed *t* tests (stop signal reaction time [RT]: $\eta^2 = 0.94$, stimulus-response mapping error: $\eta^2 = 2.34$, posterror RT slowing: $\eta^2 = 1.50$, ERN: $\eta^2 = 1.51$, FRN: $\eta^2 = 0.95$). We found that a sample size of 18 subjects is sufficient to detect an effect of the same magnitude with 80% power at the $p = 0.05$ significance level.

Stimuli and procedure. All experiments began with brain stimulation and were followed by an ERP recording. In Experiments 1, 3, and 4, each subject participated in three different stimulation conditions (i.e., anodal, cathodal, and sham) on different days with order counterbalanced across subjects. In Experiment 2 (i.e., the duration experiment), all subjects first underwent a sham stimulation session so that we could acquire neural and behavioral baselines for each subject. On a subsequent testing day, all subjects received an anodal stimulation session, followed by a 1 h break, and then another sham stimulation session. This design allowed us to determine whether the effects of anodal tDCS could last for up to 6 h. In all experiments, the time interval between testing days was >48 h, which avoids ordering confounds related to repeated brain stimulation exposure (Monte-Silva et al., 2013).

Immediately after active stimulation or sham, the subjects from Experiments 1–3 performed a two-alternative forced-choice target discrimination task in which stop signals could also occur (see Fig. 1*B*), whereas the subjects from Experiment 4 performed a simple detection version of this target discrimination task with stop signals (i.e., the target stimulus was always a black square, 10 cd/m^2, requiring a simple detection response with only one button on the gamepad). All trials of the task began with central fixation (0.37° square, 30 cd/m^2, 800–1200 ms). On all trials, a peripheral target (1° × 1°, 10° from the center of screen along the horizontal meridian, 700 ms) appeared to the left of fixation on half of the trials and to the right on the remainder of the randomly interleaved trials. On no-stop trials (66% of all trials), only the target was present. On the randomly interleaved stop trials (33% of all trials), subjects had to withhold their response when they saw the stop signal (a central square subtending 0.66°, with 0.08° line width, 30 cd/m^2). Six stop signal delays (SSDs, the stimulus-onset asynchrony between on the onset of the target and the onset of the stop signal) were sampled with equal probability: 60, 120, 180, 240, 300, and 360 ms. Previous experiments in our laboratory and others have shown this to be an effective SSD range in target discrimination tasks with results mirroring those obtained using a dynamic tracking procedure (Logan et al., 1984; Reinhart et al., 2012). Additionally, by not implementing a dynamic tracking procedure, our task avoided the restricting effects that such a method would have on the dynamics of subjects' response processes on no-stop trials, and ensured that error rates on stop trials could vary across stimulation conditions. After presentation of the stop signal, the stimuli remained on the screen until 700 ms had elapsed from the presentation of the target. The intertrial interval was 1000–1200 ms, randomly jittered with a rectangular distribution.

Adopting the established learning manipulation of Holroyd and Coles (2002), Experiments 1–3 required subjects to learn which of two buttons on the handheld gamepad to press to respond to each target color. Then, the target colors changed across days so that subjects would have to relearn the stimulus-response mapping on each day. On any given testing day, target stimuli could appear in 1 of 3 pairs of colors (red, $x = 0.612$, $y = 0.333$, 15.1 cd/m^2 and blue, $x = 0.146$, $y = 0.720$, 6.41 cd/m^2; magenta, $x = 0.295$ $y = 0.153$, 19.3 cd/m^2 and green, $x = 0.281$, $y = 0.593$, 45.3 cd/m^2; or purple, $x = 0.245$ $y = 0.126$, 9.3 cd/m^2 and yellow, $x = 0.408$, $y = 0.505$, 54.1 cd/m^2). Subjects were told that one button on the handheld gamepad was to be used to respond to one color and another button was to be used to respond to the other color presented during that session. Both buttons were pressed with the thumb of their right hand. The stimulus-response mapping assignments (i.e., which of the three color pairs and the mapping of each color to the appropriate button) were randomized across days with the order of each color-to-button set randomized across subjects. However, the subjects had to learn during the session through trial and error which button was mapped to which color. This was made more challenging by our implementation of a 700 ms deadline for any button press and the simultaneous demands of inhibiting responses to the interleaved stop signals. The competing cognitive demands of the task enabled us to stretch learning across the first 25–30 trials and allowed us to obtain enough errors to reliably measure the ERN and FRN.

To effectively establish stimulus-response mappings, subjects were provided with performance-based feedback at the end of every trial, including correct stop trials and trials in which the response deadline was missed. Feedback occurred 1000 ms after the 700 ms response window had lapsed. Feedback was in the form of a 1000 ms, centrally presented outline of a circle (0.88° diameter, 0.13° thick) or cross (0.88° length, 0.13° thick) with the meaning of these symbols (i.e., correct vs incorrect) randomized across sessions and subjects. There was no learning manipulation or feedback stimuli presented in Experiment 4. Each subject performed 1440 trials in each session interspersed with short breaks to prevent fatigue.

The tDCS was administered using a battery-driven, constant current stimulator (Mind Alive) and pair of conductive rubber electrodes (active, 19.25 cm^2; reference, 52 cm^2). The electrodes were placed in saline-soaked synthetic sponges and held in place by a headband. The reference electrode was placed on the center on the right cheek (Experiments 1, 2, and 4) or the left cheek (Experiment 3) to avoid any confounding effects from other brain regions (Berryhill et al., 2010; Hsu et al., 2011; Tseng et al., 2012). Specifically, the cheek electrode was placed diagonally, 3 cm from the cheilion (lip corner at rest) along an imaginary line connecting the cheilion to the ipsilateral condylion (palpable when the jaw is moved) (see Fig. 1*C*). Current was applied for 20 min at 1.5 mA intensity over medial–frontal cortex (site FCz, from the International 10–20 System). Comparable stimulation protocols are thought to be sufficient to create an excitatory (anodal) or inhibitory effect (cathodal) for up to 90 min in motor cortex (Nitsche and Paulus, 2001; Nitsche et al., 2003c). However, the differences between previous stimulation protocols and the present study are noteworthy. In part, the methodological differences between the present study and past work motivate Experiment 2 where we determine the duration of the effects we observe in Experiment 1. We selected the placement of stimulation at electrode site FCz because our current flow models indicated that we would influence the medial–frontal structures hypothesized to generate these medial–frontal negativities, as well as this being the site where the ERN and FRN are maximal (Gehring et al., 2012; Reinhart et al., 2012). A sham tDCS condition was administered following an identical procedure, but stimulation only lasted 30 s, ramping up and down at the beginning, middle, and end of the 20 min period, mirroring the periodic tingling sensation that subjects endorsed at stimulation sites on active testing days. Debriefing questions confirmed that

subjects were blind to the presence and polarity of stimulation, and no subject reported adverse effects of stimulation beyond mild tingling under tDCS electrodes.

During each session, subjects' ERPs were recorded using our standard procedures (Reinhart et al., 2012). The raw electroencephalogram (EEG) was acquired (250 Hz sampling rate, 0.01–100 Hz bandpass filter) using an SA Instrumentation Amplifier from 21 tin electrodes, including 3 midline (Fz, Cz, and Pz), 7 lateral pairs (F3/F4, C3/C4, P3/P4, PO3/PO4, T3/T4, T5/T6, and O1/O2), and 2 nonstandard sites (OL, midway between O1 and T5; and OR, midway between O2 and T6), arrayed according to the International 10–20 System and embedded in an elastic cap (Electrocap International). Electrode impedances were kept <5 kΩ. Signals were referenced online to the right mastoid electrode and rereferenced offline to the average of the left and the right mastoids (Nunez and Srinivasan, 2006). Horizontal eye position was monitored by recording electrooculogram (EOG) from bipolar electrodes located at the outer canthi of each eye. Vertical eye position and blinks were similarly monitored with bipolar electrodes placed above and below the left orbit. Periorbital electrodes were used to detect eye movements and a two-step ocular artifact rejection method was implemented (Woodman and Luck, 2003). One subject was replaced for excessive blinks. The ERPs were digitally filtered with a zero-phase shift, 35 Hz low-pass hamming window (SD = 6 ms) for presentation in the figures. However, we performed all statistical analyses on unfiltered data.

Data analyses: behavior. We adopted the method of Logan et al. (1984) as implemented by other researchers (e.g., Hanes et al., 1998; Godlove et al., 2011; Reinhart et al., 2012) to estimate stop signal reaction time (SSRT). In short, SSRT was estimated by one method assuming that SSRT is a constant, and by a second method assuming that SSRT is a random variable. Because there is no basis for choosing one assumption over the other, we averaged both SSRT estimates. Posterror slowing calculations accounted for the effects of nonstationarity on RT estimates (Nelson et al., 2010). For this correction, posterror slowing was calculated as the RT on no-stop trial $n + 1$ minus RT on no-stop trial $n - 1$, where n is an error after a stop signal or on a no-stop trial.

ERPs. For the ERN, error positivity (Pe), and correct-related negativity (CRN) analyses, the continuous EEG recording was time-locked to the button-press onset and baseline corrected to the interval from 200 to 50 ms before response. The baseline interval ended 50 ms before the time-locking event to allow these analyses to reveal error-related activity starting before response onset (Gehring et al., 2012). For the FRN analysis, EEG was time locked to the onset of the external feedback stimuli and baseline corrected from 200 to 0 ms before feedback. For P1 and N1 analyses, EEG was locked to target onset and baseline corrected 200 to 0 ms before target. For the lateralized-readiness potential (LRP) analysis, EEG was locked to button-press onset, baseline corrected 800 to 600 ms before response (Smulders and Miller, 2012). For the analysis of the responses to the stop signals, previously described as the central or stop-signal N2 (Luck and Hillyard, 1990; Pliszka et al., 2000; Schmajuk et al., 2006), EEG was locked to stop-signal stimuli on correct stop trials and baseline corrected from 200 to 0 ms before stop-signal onset. Stop trials on which subjects responded before stop signals were presented were not included in ERN analyses because subjects did not have the necessary information to deduce that an error had been committed. When constructing grand average ERP waveforms collapsed across left and right target locations, the number of trials presented at each location was matched in a given condition by excluding random trials from the more heavily represented target with the behavior of interest. Because of the lateralized nature of P1 and N1 components in this paradigm, data were collapsed across left and right target locations and averaged using a procedure that preserved the electrode location relative to the target location.

The ERN and FRN amplitudes were measured from midline electrodes (Fz, Cz, and Pz) using a time window from −50 to 150 ms relative to the response onset and 200–400 ms relative to the feedback onset, respectively. We calculated amplitude of the voltages as the mean area under the curve of the difference wave subtracting errant no-stop trials from correct no-stop trials (Gehring et al., 2012). The Pe was measured as the maximum amplitude on no-stop error trials, 200–400 ms after response onset at the midline parietal electrode (Pz) (Gehring et al., 2012). The P1 (measured from electrodes OR and OL, from 100 to 150 ms after target onset), N1 (measured from electrodes OR and OL, from 150 to 200 ms after target onset), and N2 (measured from electrode Cz, from 175 to 225 ms after stop-signal onset) amplitudes quantified as mean values during the time windows, consistent with previous research (Luck and Hillyard, 1990; Pliszka et al., 2000; Schmajuk et al., 2006). Latency was measured using peak amplitude in each measurement window for each component. The LRP was measured from central lateral electrodes (C3/C4) during the time window from −200 to 0 ms relative to response onset as contralateral − ipsilateral waveforms with respect to the right hand used for the button-press responses (Smulders and Miller, 2012). It should be noted that the LRP we measured was untraditional because of our use of responses made by a single hand to avoid Simon-effect interference from the lateralized targets. The LRP amplitude was defined as mean voltage in the window from LRP onset until response, and the LRP onset latency was defined as the time point at which the voltage reached 50% of the peak amplitude (Miller et al., 1998; Kiesel et al., 2008).

The signal-to-noise ratio was calculated by statistically estimating the total power of the signal and the noise using the following equations:

$$P_{noise} = \frac{\sum_{n=1}^{n=N}\sum_{k=1}^{k=K}(x_{kn} - \bar{x})^2}{K * N - 1}$$

$$P_{signal} = \frac{\sum_{n=1}^{n=N}\sum_{k=1}^{k=K} x_{kn}^2}{K * N} - P_{noise}$$

$$SNR = \frac{P_{signal}}{P_{noise}}$$

where P_{noise} is noise power, P_{signal} is signal power, K is the number of data points in a segment, N is the number of segments, and x is EEG amplitude. Similar methods are used in ERP research (e.g., Clayson et al., 2013). It is assumed that the signal and noise are uncorrelated and that the average power of the signal is equal to the difference between the average total power and the average noise power.

We entered the ERN and FRN amplitudes into within-subjects ANOVAs with the factors of condition (anodal vs sham vs cathodal), trial type (correct vs error), and electrode site (Fz vs Cz vs Pz). In addition, we used preplanned two-tailed t tests for simple comparisons between each tDCS condition versus sham. ANOVAs with the factors of condition (anodal vs sham vs cathodal) and trial bin (bin 1 vs bin 2 vs bin 3 vs bin 4) were used for learning analyses. Separate bin-wise analyses were performed for each dependent variable of RT, accuracy (in percentage correct), ERN and FRN values averaged into 4 bins of 10 trials each (i.e., bin 1 contained trials 1–10, bin 2 contained trials 11–20, etc.) consistent with previous work (Holroyd and Coles, 2002). Interactions were parsed with follow-up ANOVAs. We adjusted p values using the Greenhouse-Geisser ε correction for nonsphericity when this assumption was violated (Jennings and Wood, 1976). Finally, we used median and range as measures of central tendency and variability in the follow-up experiment examining the right versus left laterality of tDCS reference electrode (i.e., Experiment 3) because of a smaller sample size ($N = 10$). In this experiment, we used the Wilcoxon Signed Ranks Test for comparison between pairs of variables (e.g., within-condition contrasts between error and correct trials); and for the nonparametric alternative to the ANOVA with repeated measures, we used the Friedman's two-way ANOVA by ranks.

Current-flow model. Our model of tDCS current flow was informed by previously established methods (De Lucia et al., 2007; Wagner et al., 2007b; Sadleir et al., 2010). This involved (1) MRI segmentation, (2) electrode placement, (3) generation of a finite element model, and (4) computation. We used the MNI T1-weighted MRI reference brain from the CURRY 6.0 multimodal neuroimaging software (Compumedics Neuroscan). A combination of automated and manual segmentation tools was used to obtain tissue masks, including Gaussian filters, and morphological and Boolean operations implemented in MATLAB (MathWorks). Volumetric mesh was generated from the segmented data ($>$140,000 vertices, $>$800,000 tetrahedral elements). Segmented compartments and their respective isotropic electrical conductivities (in S/m) included: skin (0.33), skull (0.0042), and brain (0.33).

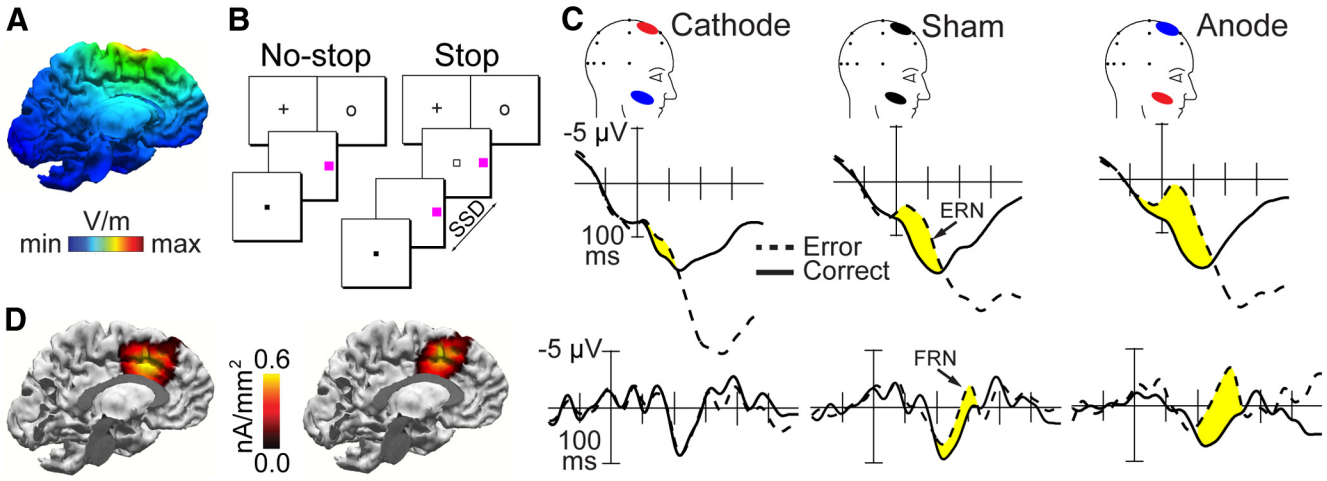

Figure 1. Task, tDCS model, and primary electrophysiological results from Experiment 1. ***A***, The modeled distribution of current during active tDCS on a medial–sagittal view of a 3D reconstruction of the cortical surface. ***B***, The target discrimination task with stop signals requiring subjects to report the color of the target (red vs blue, magenta vs green, or purple vs yellow) by pressing one of two buttons on a handheld gamepad unless a stop signal appeared at a variable SSD after target onset. ***C***, Response-locked and feedback-locked grand average ERPs from correct (solid line) and errant (dashed line) no-stop trials shown at the central midline electrode (Cz) across conditions. The yellow shaded regions represent the latency windows of the ERN (top) and FRN (bottom). ***D***, Current density distribution models of the ERN (left) and FRN (right) shown on medial–sagittal 3D reconstructions of the cortical surface in the sham condition. Warmer colors represent greater current flow.

Our forward computation used a finite element model, implemented in SCIRun (available as open source software: http://software.sci.utah.edu). We simulated normalized current flow using a bipolar electrode configuration with the anode (19.25 cm^2) centered over FCz, and the cathode (52 cm^2) centered over the right cheek between the zygomaticus major and the condylion. The left cheek was used for our follow-up experiment using this electrode configuration. Current density corresponding to 1.5 mA total current was applied at the anode electrode and ground was applied at the negative electrode.

The Laplace equation. $\vec{\nabla} \cdot (\sigma \vec{\nabla} \varphi) = 0$. ($\varphi$, potential; σ, conductivity) was solved, and the following boundary conditions were used. Inward current flow = J_n (normal current density) was applied to the exposed surface of the anode electrode. The ground was applied to the exposed surface of the cathode electrode. All other external surfaces were treated as insulated. Plots showing the course of electrical field magnitude through brain tissue were generated in MATLAB.

Current-density model. Using the same volume conductor model described above for our forward model, we computed current density models of subjects' response- and feedback-locked ERPs. The standardized low-resolution electromagnetic tomography (sLORETA) weighted accurate minimum norm method (SWARM) was estimated using electrode positions based on the International 10–20 System. SWARM combines the methods of diagonally weighted minimum norm least squares (Dale and Sereno, 1993) and sLORETA (Pascual-Marqui, 2002) to compute a current density vector field (Wagner et al., 2007a). This electrical field modeling was based on the grand average ERP difference waves (i.e., no-stop error − no-stop correct) during the ERN (−50 to 150 ms) and FRN measurement windows (200–400 ms) using the entire array of electrodes. Although distributions of reconstructed current density provide an estimate of the location of neuronal generation of ERPs, they provide no definitive information about the neural origins of these ERPs (Luck, 2005; Woodman, 2010).

Results

First, we describe the results from the principal experiment (i.e., Experiment 1). Then, we describe the results from several follow-up experiments designed to examine the duration of the primary effects (Experiment 2), rule out alterative interpretations of the results (Experiment 3), and extend the findings to a task with fewer competing cognitive demands (Experiment 4).

Experiment 1: error- and feedback-related negativities

We found that switching the direction of the current flow switched the direction of the causal effects on the medial–frontal

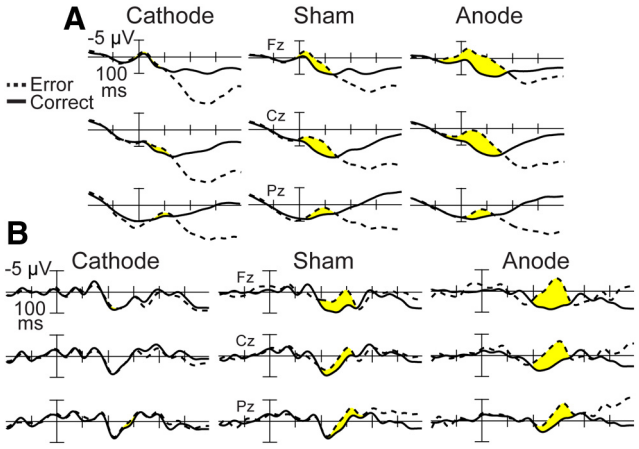

Figure 2. tDCS effects on medial–frontal negativities from Experiment 1. Grand average ERP waveforms from correct no-stop trials (black line) and errant no-stop trials (dashed line) aligned to response (***A***) and feedback events (***B***) shown at each midline electrode site (Fz, Cz, and Pz) for cathodal, sham, and anodal conditions from Experiment 1. Shaded yellow regions represent the latency window of the ERN (−50 to 150 ms relative to response onset) and FRN (200 – 400 ms relative to feedback onset).

negativity elicited by errors (i.e., the ERN) and by negative feedback (i.e., the FRN; Fig. 1*C*; see below for a detailed discussion of this feedback-locked ERP effect). After cathodal stimulation, the ERN and FRN were essentially eliminated such that there was no significant difference in the waveforms between correct and error responses ($t_{(17)} = 1.27$, $p = 0.22$), or positive and negative feedback ($t_{(17)} = 0.81$, $p = 0.43$). Consistent with this observation, the amplitude of the ERN and FRN was significantly reduced relative to those measured in the sham condition with the same subjects (ERN $t_{(17)} = 3.85$, $p < 0.01$, FRN $t_{(17)} = 4.33$, $p < 0.01$; for additional details, see Figs. 2 and 3). In contrast, after anodal stimulation, the ERN and FRN amplitudes were almost twice that observed in the sham condition (ERN $t_{(17)} = 3.58$, $p < 0.01$, FRN $t_{(17)} = 4.50$, $p < 0.01$). Consistent with our ability to control the amplitudes of the ERN and FRN, the current-density models of these medial–frontal negativities overlap with the current flow model of the tDCS (compare Fig. 1*A*,*D*). Previous correlational

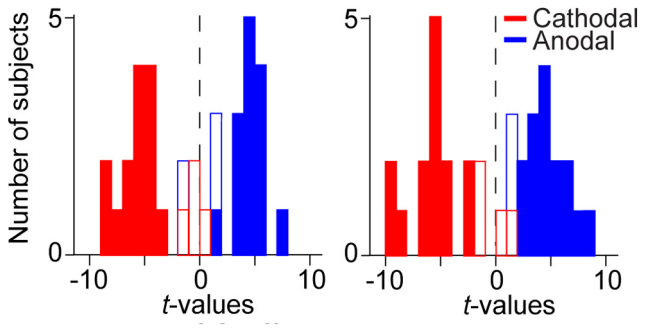

Figure 3. tDCS effects on individual subject medial–frontal negativities from Experiment 1. *t* values from each subject aggregated into a frequency distribution to illustrate variability in the bidirectional effects of tDCS on the medial–frontal negativities across subjects from Experiment 1. *t* values are based on comparisons between anodal versus sham (blue) and cathodal versus sham (red) using single-subject ERN amplitude (left) or FRN amplitude (right). Significant *t* values are shown in solid color (*t* test, two-tailed, $p < 0.05$).

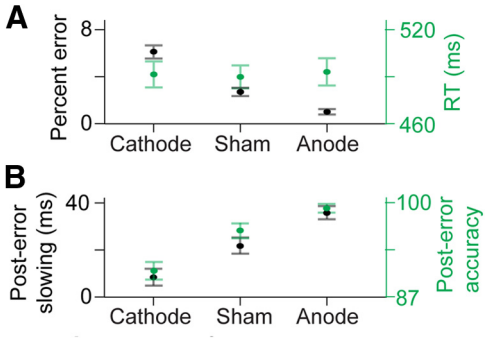

Figure 4. Behavior from Experiment 1. ***A***, Mean percentage of stimulus response mapping errors on no-stop trials and mean RT on no-stop trials across conditions. ***B***, Posterror slowing of RT and accuracy after a failure to stop or a failure to map a stimulus to the correct response shown across conditions. Error bars indicate SEM.

studies suggested that the medial–frontal cortex could be the source of the ERN and FRN (Gehring and Willoughby, 2002; Ito et al., 2003), and our causal manipulations provide converging support for this proposal. In sum, cathodal stimulation of medial–frontal cortex nearly eliminated the normal electrophysiological activity related to human performance monitoring, whereas anodal stimulation significantly boosted this activity.

To further examine the effects of medial–frontal stimulation on the amplitudes of the ERN and FRN, we analyzed these waveforms across the midline electrode sites as a function of tDCS condition. Figure 2 shows that tDCS up- and down-regulated the amplitude of the ERN and FRN with a cathodal < sham < anodal pattern. To confirm these observations statistically, we computed within-subjects ANOVAs with the factors of condition (anodal vs sham vs cathodal), trial type (correct vs error), and electrode site (Fz vs Cz vs Pz) on the amplitude of the ERN (−50 to 150 ms) and FRN (200–400 ms). For both components, there were three-way interactions of condition × trial type × electrode site (ERN $F_{(4,68)} = 3.492, p < 0.03$, FRN $F_{(4,68)} = 2.61, p < 0.05$). Follow-up ANOVAs showed main effects of trial type and a trial type × electrode site interaction for sham (ERN $F_{(1,17)} = 20.09, p < 0.01$, $F_{(2,34)} = 4.92, p < 0.02$, FRN $F_{(1,17)} = 28.24, p < 0.01$, $F_{(2,34)} = 3.74, p < 0.03$) and anodal conditions (ERN $F_{(1,17)} = 196.65, p < 0.01$, $F_{(2,34)} = 45.40, p < 0.01$, FRN $F_{(1,17)} = 86.71, p < 0.01$, $F_{(2,34)} = 5.51, p < 0.01$), but not for the cathodal condition (ERN $F_{(1,17)} = 0.28, p = 0.60$, $F_{(2,34)} = 1.36, p = 0.27$, FRN $F_{(1,17)} = 0.39, p = 0.54$, $F_{(2,34)} = 0.59, p = 0.51$). It is noteworthy to point out that similar results were obtained if the ERN and FRN waveforms were derived from errant stop trials.

These results demonstrate three findings: (1) that errant responses and error-feedback stimuli elicited more negative potentials (i.e., the ERN and FRN) after sham (ERN $t_{(17)} = 2.53, p < 0.03$, FRN $t_{(17)} = 2.32, p < 0.04$) and anodal stimulation (ERN $t_{(17)} = 11.25, p < 0.01$, FRN $t_{(17)} = 9.89, p < 0.01$); (2) that ERNs and FRNs after sham (ERN $t_{(17)} = 4.22, p < 0.01$, FRN $t_{(17)} = 2.73, p < 0.02$) and anodal conditions (ERN $t_{(17)} = 8.54, p < 0.01$, FRN $t_{(17)} = 3.16, p < 0.01$) were largest at anterior electrode sites relative to the posterior sites, the known distribution of these components (e.g., Reinhart et al., 2012); and (3) that the largest ERNs and FRNs were observed after anodal stimulation, whereas the smallest ERNs and FRNs followed cathodal stimulation (i.e., cathodal < sham < anodal). To summarize, errors elicited the expected medial–frontal negativities in the sham condition, with the familiar distribution of effects shown across frontal, central, and parietal midline electrode sites. Critically, cathodal stimulation over medial–frontal cortex in the same subjects completely eliminated these neural signatures of performance monitoring, whereas anodal stimulation over the same region increased the amplitudes of these components.

The tDCS bidirectional effects on the medial–frontal negativities were consistent across subjects. Figure 3 shows the cross-subject variability in the bidirectional effects of tDCS on the ERN and FRN. A majority of subjects (14 of 18 for both conditions) exhibited significant ERN amplitude enhancement after anodal stimulation (*t* test, two-tailed, $p < 0.05$, *t* value, mean ± SEM, 3.65 ± 0.6) and significant reduction after cathodal stimulation (*t* value, mean ± SEM, −4.44 ± 0.6). Similarly, a majority of subjects (anodal, 15 of 18; cathodal, 14 of 18) showed the same pattern of results for the amplitude of the FRN (anodal, 4.16 ± 0.5; cathodal, −4.12 ± 0.7). In sum, we observed bidirectional effects of tDCS on the performance-monitoring electrophysiology in the vast majority of our sample (~75% of the individual subjects), emphasizing the between-subjects reliability of these findings.

Experiment 1: behavior

The bidirectional changes in neural activity were paralleled by similarly bidirectional changes in the behavioral responses of the subjects to the targets. As shown in Figure 4*A* (see also Table 1), we found that, when the medial–frontal potentials were eliminated by cathodal stimulation, the error rates increased without changing RTs relative to sham. In contrast, doubling the amplitude of these potentials with anodal stimulation caused error rates to be cut in half without any accompanying change in RTs. Specifically, subjects made significantly more errors responding to the target colors on no-stop trials after cathodal stimulation ($t_{(17)} = 3.59, p < 0.01$) and significantly fewer errors after anodal stimulation ($t_{(17)} = 3.76, p < 0.01$) relative to sham. Moreover, Figure 5 shows that individuals with the greatest anodal-induced gains in ERN ($r_{(16)} = -0.543, p < 0.02$) and FRN ($r_{(16)} = -0.469, p < 0.05$) amplitude showed the most improvements in no-stop accuracy (i.e., decreased error rates), whereas subjects with the largest cathodal-induced reductions in ERN ($r_{(16)} = -0.538\ p < 0.03$) and FRN ($r_{(16)} = -0.471, p < 0.05$) amplitude committed the most number of errors. These changes in stimulus-response mapping errors were not due to subjects simply failing to respond (probability of responding on no-stop trials, mean ± 95% within-subjects confidence interval, cathodal 97.2 ± 0.9, sham 96.6 ± 1.3, anodal 96.5 ± 1.4, $p > 0.2$), or to changes in RTs across stimulation conditions (Fig. 4A; $p > 0.4$) as mean RTs on

Table 1. Errors across stimulation conditions and experiments[a]

	Anodal		Sham		Cathodal	
	No-stop	Stop	No-stop	Stop	No-stop	Stop
Experiment 1	1.09 ± 0.11	48.2 ± 3.2	2.56 ± 0.43	50.9 ± 1.3	6.24 ± 0.70	54.2 ± 4.0
Experiment 2	1.27 ± 0.20	47.9 ± 1.8	2.44 ± 0.37	50.8 ± 1.6	—	—
Experiment 3	1.02 ± 0.14	49.2 ± 2.0	2.37 ± 0.49	50.0 ± 1.0	5.37 ± 0.68	53.2 ± 2.4
Experiment 4	—	48.3 ± 3.5	—	51.2 ± 1.9	—	54.1 ± 3.6

[a]Mean percentage of stimulus-response mapping errors on no-stop trials, and mean percentage of inhibition errors on stop-signal trials across stimulation conditions and experiments. —, Not applicable.

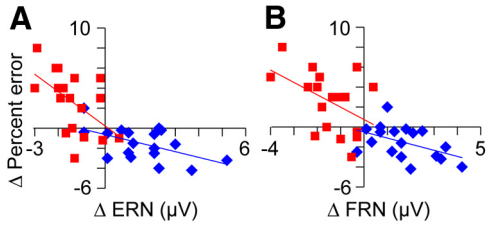

Figure 5. tDCS induced brain-behavior correlations from Experiment 1. ***A***, The relationship between individual subjects' mean percentage of no-stop errors and mean ERN amplitude as anodal-minus-sham (blue) and cathodal-minus-sham (red) difference scores. ***B***, Scatter plots are as in ***A*** using mean FRN amplitude.

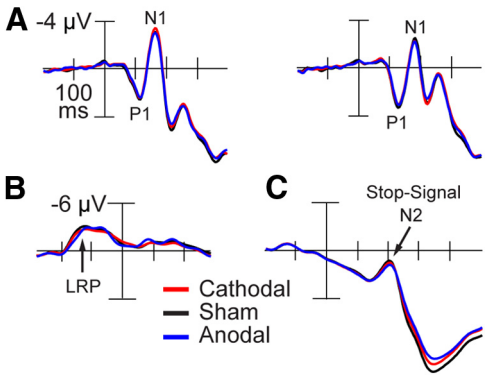

Figure 6. Perceptual, response, and stop signal ERPs from Experiment 1. ***A***, Target-locked grand average potentials from correct, no-stop trials shown at lateral occipitotemporal sites (OL/OR) contralateral (left) and ipsilateral (right) with respect to target location recorded during the sham (black), cathodal (red), and anodal (blue) conditions. Labels show P1 and N1 components. ***B***, Response-locked grand average difference waves (contralateral − ipsilateral with respect to response hand) at central lateral electrodes (C3/C4) from correct no-stop trials across conditions as in ***A***. Arrow indicates the LRP. ***C***, Stop signal-locked grand average potentials on correct stop trials at the central midline electrode (Cz) across conditions as in ***A***. Arrow indicates the prominent negativity (previously termed the stop-signal N2 component).

correct no-stop trials were uninfluenced by the stimulation. This shows that the changes in accuracy were not simply due to subjects trading speed for accuracy across the different stimulation conditions.

Cognitive control theories attribute posterror slowing to adaptive control mechanisms that induce more careful behavior to reduce the probability of error commission (e.g., Rabbitt and Rodgers, 1977; Brewer and Smith, 1989; Cohen et al., 2000; Botvinick et al., 2001). If medial–frontal stimulation changes the operation of an adaptive control mechanism, then we should see costs and benefits in the compensatory behavior on trials after an error. This is precisely the pattern of results we observed. Subjects' posterror slowing was cut in half after cathodal ($t_{(17)} = 2.56$, $p < 0.02$) and doubled after anodal stimulation ($t_{(17)} = 4.35$, $p < 0.01$) relative to the significant posterror slowing after sham tDCS ($t_{(17)} = 3.68$, $p < 0.01$) (Fig. 4*B*). Subjects also made a correct response on the trial after an error more frequently after anodal ($t_{(17)} = 3.88$, $p < 0.01$) and less frequently after cathodal stimulation ($t_{(17)} = 5.17$, $p < 0.01$) relative to sham (Fig. 4*B*).

Our tDCS manipulations were relatively selective in that they only influenced the widely accepted markers of cognitive control reported above (i.e., posterror slowing and error rate) and not a variety of other behavioral measures. For example, the probability of any incorrect response on a stop trial did not significantly differ across stimulation conditions (mean ± 95% within-subjects confidence interval, cathodal 54.2 ± 4.0, sham 50.9 ± 1.3, anodal 48.2 ± 3.2, $p > 0.09$). Similarly, analyses of SSRT, an index of how quickly a planned response can be shut down, showed that the amount of time subjects needed to successfully stop was not significantly affected by tDCS (mean ± 95% within-subjects confidence interval, cathodal 224.9 ± 7 ms, sham 219.3 ± 6 ms, anodal 215.3 ± 7 ms, $p > 0.13$). That our tDCS protocol appears to discriminate between categories of behavioral errors is consistent with the dissociation often drawn between different types of errors, particularly stop versus no-stop errors (Verbruggen and Logan, 2008; Verbruggen et al., 2008; van Driel et al., 2012; Schroder and Infantolino, 2013). However, it is noteworthy that our stimulation protocol had trend-level effects on stop-trial behavior. In sum, tDCS effects on RT and accuracy after an error provide causal support for the view that the medial–frontal activity underlying the ERN and FRN performs error monitoring (Falkenstein et al., 1990; Gehring et al., 1993; Miltner et al., 1997) and is necessary to exert cognitive control by slowing processing after an error (Rabbitt, 1966; Laming, 1968).

Experiment 1: perceptual, response, and stop signal ERPs

The results we have shown so far would hardly be surprising if our stimulation influenced stages of cognitive processing before error detection. For example, if the medial–frontal tDCS affected perceptual processing or preparation of the manual button-press responses, then the behavioral effects could be attributed to modulations of mechanisms that operate before the medial–frontal ERN and FRN. We examined the effects of our tDCS on other ERP components beginning with the earliest sensory and perceptual potentials (Eason et al., 1969; Van Voorhis and Hillyard, 1977) and continuing through to the ERP components related to response processes. Figure 6*A* shows that the P1 and N1 elicited by the target stimuli were unaffected by the stimulation (for the statistical results, see Table 2). Next, we tested for differences across stimulation conditions on the response-locked ERPs from correct no-stop trials (i.e., the LRP and CRN) and the stop signal-locked ERPs on correct stop trials (i.e., the stop-signal N2). We found that our tDCS manipulations left all these ERP components unchanged (Figs. 1*C* and 6*B*,*C*), as evidenced by no main effects of condition on amplitude (LRP $F_{(2,34)} = 0.30$, $p = 0.69$; CRN $F_{(2,34)} = 1.22$, $p = 0.31$; N2 $F_{(2,34)} = 0.76$, $p = 0.46$) or latency (LRP $F_{(2,34)} = 0.53$, $p = 0.58$; CRN $F_{(2,34)} = 0.12$, $p = 0.83$; N2 $F_{(2,34)} = 0.35$, $p = 0.69$). These findings demonstrate the selectivity of medial–frontal tDCS in changing only electrophys-

Table 2. P1 and N1 statistical results from Experiment 1[a]

	F, *p*
Contralateral	
P1 amplitude	$F_{(2,34)} = 0.05, p = 0.87$
P1 latency	$F_{(2,34)} = 0.49, p = 0.62$
N1 amplitude	$F_{(2,34)} = 1.92, p = 0.16$
N1 latency	$F_{(2,34)} = 0.06, p = 0.92$
Ipsilateral	
P1 amplitude	$F_{(2,34)} = 0.50, p = 0.47$
P1 latency	$F_{(2,34)} = 0.36, p = 0.62$
N1 amplitude	$F_{(2,34)} = 0.46, p = 0.62$
N1 latency	$F_{(2,34)} = 0.33, p = 0.66$

[a]No main effect of condition was observed in the amplitude or latency analyses of the P1 and N1 ERP components, contralateral and ipsilateral with respect to target location.

iological responses of the ERN and FRN, but not changing the operation of cognitive mechanisms indexed by other components.

Experiment 1: medial–frontal activity and learning

Above we found evidence supporting the idea that medial–frontal activity enables executive control of cognition through reactions to an error-detection mechanism; however, a more recent view states that this activity underlies our ability to rapidly learn new tasks (Holroyd and Coles, 2002; Brown and Braver, 2005; Alexander and Brown, 2011). According to this view, actions and events are linked to their outcomes by a reward prediction error signal to the response (i.e., the ERN) and a reward prediction error signal to the feedback (i.e., the FRN), which are both associated with the arrival of phasic dopamine in the anterior cingulate of medial cortex (Holroyd and Coles, 2002).

The learning account of medial–frontal cortex proposes that the information needed to generate an error signal early in learning will only be available at the end of a trial when external feedback is provided, whereas later in learning the brain will detect the error at the time of the response and will not need to wait for the feedback. This results in the prediction that we should observe smaller ERN amplitudes and larger FRN amplitudes early in learning, but larger ERN amplitudes and smaller FRN amplitudes later as learning establishes the contingencies between stimuli, responses, and feedback (Holroyd and Coles, 2002; Brown and Braver, 2005). Our findings from the sham condition are consistent with the learning account of the medial–frontal negativities. We observed that the ERN elicited by an error response grew progressively larger, whereas the FRN elicited by negative feedback grew progressively smaller (Fig. 7*A*,*B*). These observations were confirmed statistically by main effects of trial bin on ERN ($F_{(3,51)} = 8.93, p < 0.01$) and FRN amplitude ($F_{(3,51)} = 4.29, p < 0.04$). As subjects learned the stimulus-response mappings in the sham condition (Fig. 7*C*,*D*), RT sped up ($F_{(3,51)} = 25.68, p < 0.01$) and accuracy increased ($F_{(3,51)} = 26.15, p < 0.01$).

If our medial–frontal stimulation changed the neural signals used in learning (i.e., the ERN and FRN across trials), then we also should have changed subjects' learning rates with tDCS. Figure 7*A–D* shows that with cathodal stimulation we slowed the rate of learning, whereas with anodal stimulation we sped up the rate of learning. This was demonstrated by interactions of stimulation condition × trial bin on ERN amplitude ($F_{(3,51)} = 7.20, p < 0.01$) and FRN amplitude ($F_{(3,51)} = 4.64, p < 0.02$), as well as RT (no-stop trial mean RT, $F_{(3,51)} = 3.80, p < 0.05$) and accuracy (no-stop trial percentage correct, $F_{(3,51)} = 5.09, p < 0.02$). Additionally, by fitting these learning data with a power function to model learning rates, we found that cathodal stimulation reduced the rate parameters of the ERN ($t_{(17)} = 3.86, p < 0.01$), FRN ($t_{(17)} = 2.45, p < 0.03$), and RTs ($t_{(17)} = 2.43, p < 0.03$) relative to sham, whereas anodal stimulation increased the rate parameters of the ERN ($t_{(17)} = 4.35, p < 0.01$), FRN ($t_{(17)} = 2.63, p < 0.02$), RT ($t_{(17)} = 2.45, p < 0.03$), and accuracy ($t_{(17)} = 2.25, p < 0.04$). Thus, our causal manipulation of medial–frontal cortex exerted bidirectional control over the rate of learning, consistent with learning models of medial–frontal cortex; most notably, we found that anodal tDCS increased the rate of learning across behavioral and electrophysiological metrics in our healthy young adults.

Experiments 1 and 2: duration of medial–frontal stimulation effects

In Experiment 1, we found that the effects of anodal tDCS on the indices of performance monitoring lasted throughout the full 2 h neurophysiological recording session. Figure 8 illustrates the within-session dynamics of mean ERN and FRN amplitudes, posterror slowing, and error rate sorted in 100 trial-wide bins (i.e., ~10 min per bin) for each stimulation condition (i.e., cathodal, sham, anodal) from Experiment 1. We observed stable bidirectional effects of tDCS across the entire recording period. To confirm statistically, we computed within-subjects ANOVAs for each neural and behavioral measure with the factors of condition (anodal vs sham) and time (bins 1–14). Main effects of condition revealed that anodal tDCS increased the amplitude of the ERN ($F_{(1,17)} = 16.80, p < 0.01$) and FRN ($F_{(1,17)} = 14.43, p < 0.01$), prolonged posterror slowing ($F_{(1,17)} = 18.78, p < 0.01$), and decreased error rate ($F_{(1,17)} = 14.92, p < 0.01$). The same analyses using the cathodal versus sham data revealed the opposite effects: tDCS reduced the amplitude of the ERN ($F_{(1,17)} = 12.84, p < 0.01$) and FRN ($F_{(1,17)} = 18.36, p < 0.01$), shortened posterror slowing ($F_{(1,17)} = 6.55, p < 0.02$), and increased error rate ($F_{(1,17)} = 11.79, p < 0.01$) relative to sham. Next, we analyzed the same data using two-tailed *t* tests to detect significant deviations between stimulation conditions (anodal vs sham and cathodal vs sham) at each of the 14 individual 10-min-long time points. We found that a majority of time points exhibited significant (i.e., $p < 0.05$) differences for comparisons between anodal and sham (ERN 12 of 13 time points, $t > 2.15$, FRN 11 of 13 time points, $t > 2.78$, posterror slowing 11 of 13 time points, $t > 2.08$, error rate 11 of 13 time points, $t > 3.10$) and between cathodal and sham conditions (ERN 13 of 13 time points, $t > 2.32$, FRN 12 of 13 time points, $t > 2.60$, posterror slowing 11 of 13 time points, $t > 3.05$, error rate 12 of 13 time points, $t > 2.39$). These results show the stability and enduring nature (longer than 2 h) of the positive and negative after-effects caused by our medial–frontal tDCS protocol in our healthy human subjects.

To determine the stability and duration of the effects of medial–frontal stimulation on the mechanisms of performance monitoring, we ran another within-subjects tDCS and ERP experiment (Experiment 2). The broadly cited estimate of a 90 min duration of tDCS is derived from research on human motor cortex using a stimulation protocol of 1 mA polarization for 5–15 min (Nitsche and Paulus, 2000, 2001; Nitsche et al., 2003a, b). In contrast, the current study targeted medial–frontal cortex and potentially more sensitive executive mechanisms. We also used a stimulation protocol of 1.5 mA polarization for 20 min. Given these differences in targeted function, brain region, and stimulation parameters, we sought to determine precisely how long the effects lasted after the administration of medial–frontal tDCS. Our duration experiment (Experiment 2) was identical to the

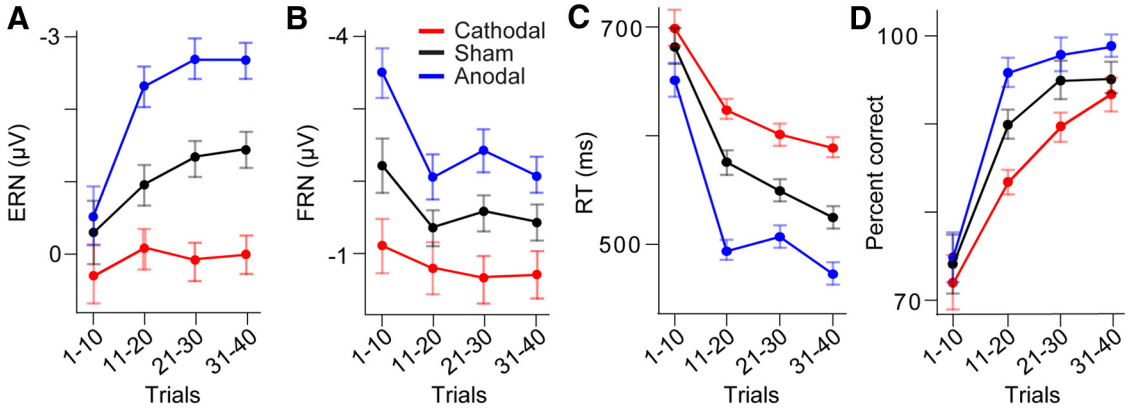

Figure 7. The effects of tDCS on learning. Mean amplitude of the ERN (***A***) and FRN (***B***). Mean RT (***C***) and accuracy (***D***) from no-stop trials sorted into 10 trial-wide bins from the start of Experiment 1 across cathodal (red), sham (black), and anodal conditions (blue). Error bars indicate SEM.

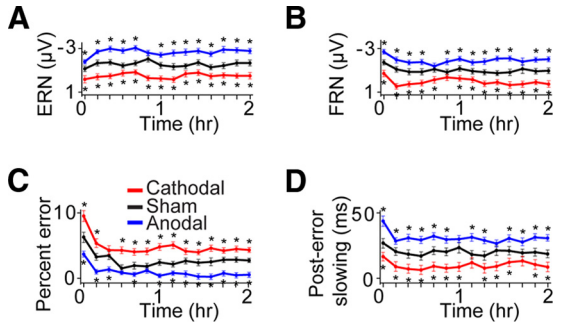

Figure 8. Duration of tDCS effects across the 2 h sessions. Mean amplitude of the ERN (***A***) and FRN (***B***) sorted into 14 sequential bins (~10 min or 100 trials per bin) shown across cathodal (red), sham (black), and anodal conditions (blue) from Experiment 1. Mean percentage of stimulus-response mapping errors on no-stop trials (***C***), and mean posterror slowing of RT after a failure to stop or a failure to map a stimulus to the correct response (***D***) binned as in ***A*** and ***B*** and shown across conditions from Experiment 1. Error bars indicate SEM. *$p < 0.05$, significant difference between the cathodal and sham or anodal and sham conditions at single time points (*t* test, two-tailed, paired samples).

primary experiment (Experiment 1) except that it differed in the order of the tDCS conditions and focused only on the beneficial cognitive effects of anodal stimulation (Fig. 9*A*).

The findings of Experiment 2 are shown in Figure 9*B–E*, representing mean ERN, FRN, posterror slowing, and no-stop error rate in 100 trial-wide bins across each successive recording session (i.e., sham, followed by anodal, followed by sham). The behavioral and electrophysiological findings from this experiment replicated all of the findings from the anodal and sham conditions of Experiment 1 (Tables 1 and 3). We observed stable anodal-induced enhancements throughout the full 2 h recording period (ERN 13 of 13 time points, $t > 3.47$; FRN 12 of 13 time points, $t > 3.52$; posterror slowing 10 of 13 time points, $t > 2.03$; error rate 10 of 13 time points, $t > 2.16$). Interestingly, each neural and behavioral measure gradually returned to their respective baseline levels after ~4.8 h after the end of anodal stimulation. That is, almost 5 h after the beneficial effects of anodal tDCS began, subjects' neural and behavioral indices of performance monitoring and executive control were no longer significantly different ($p > 0.05$) from those collected on their first day after sham stimulation. These results show that we can now causally enhance executive control processes in humans with relatively long-lasting effects using a single 20 min session of noninvasive brain stimulation over medial–frontal cortex.

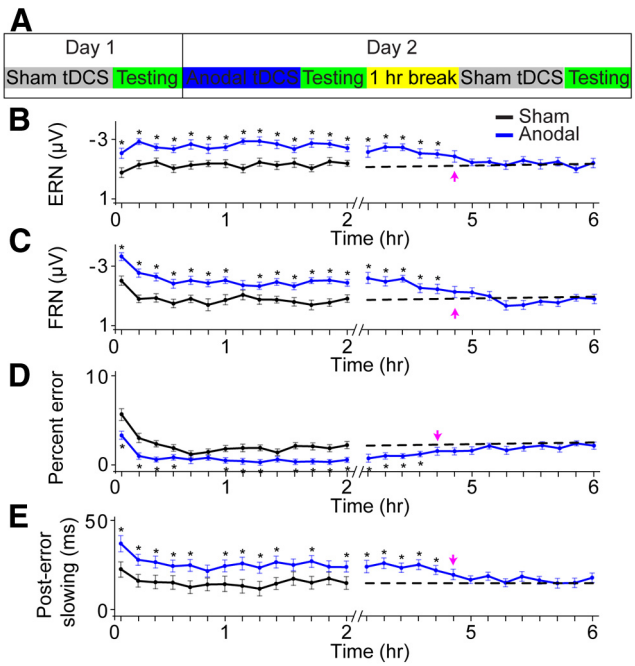

Figure 9. Duration of tDCS effects across 6 h. Schematic illustration of the experimental design from Experiment 2 (***A***). Each subject underwent a 2 day experiment. On the first day, subjects received sham stimulation over medial–frontal cortex before ERP and behavioral data collection (i.e., testing). On the second day, subjects first received anodal stimulation over medial–frontal cortex followed by testing. Subjects then waited 1 h before undergoing a final session of sham stimulation followed by testing. Mean amplitude of the ERN (***B***) and FRN (***C***), mean percentage of stimulus-response mapping errors on no-stop trials (***D***), and mean posterror RT slowing from stop and no-stop trials (***E***) sorted into 100 trial-wide bins (~10 min per bin) shown for each testing session. Solid black lines indicate data from day 1 after sham stimulation. Blue lines indicate data from day 2 immediately after anodal stimulation (left, 0–2 h) and several hours later (right, 4–6 h). Dashed black lines indicate an average of the data collected from day 1 after sham stimulation (i.e., baseline levels). The line break on the *x*-axes indicates the passage of 2 h (i.e., 1 h break, 40 min ERP setup, 20 min sham stimulation). Error bars indicate SEM. *$p < 0.05$, significant differences between conditions at single time points (*t* test, two-tailed, paired samples). Magenta arrows indicate the time point at which a measure was no longer significantly different from baseline ($p > 0.05$, followed by at least 2 consecutive nonsignificant time points).

Experiments 3 and 4: replications and extensions

We performed additional experiments to determine the robustness and reliability of our causal manipulations of medial–frontal activity and behavior. First, we found the same pattern of results on the ERN and FRN whether the right or the left cheek was used

Table 3. Statistical results comparing day 1 sham to day 2 anodal conditions from Experiment 2[a]

Category	*t*, *p*
A	
ERN amplitude	$t_{(17)} = 5.01, p < 0.01$
FRN amplitude	$t_{(17)} = 4.88, p < 0.01$
No-stop errors	$t_{(17)} = 3.12, p < 0.01$
Posterror slowing	$t_{(17)} = 3.58, p < 0.01$
Posterror accuracy	$t_{(17)} = 3.66, p < 0.01$
No-stop RT	$t_{(17)} = 0.63, p = 0.54$
B	
ERN amplitude	$t_{(17)} = 2.42, p < 0.03$
FRN amplitude	$t_{(17)} = 2.34, p < 0.04$
No-stop errors	$t_{(17)} = 2.38, p < 0.03$
No-stop RT	$t_{(17)} = 2.25, p < 0.04$
C	
SSRT	$t_{(17)} = 0.94, p = 0.36$
P (respond/stop)	$t_{(17)} = 1.33, p = 0.20$
P (respond/no-stop)	$t_{(17)} = 1.10, p = 0.29$
LRP amplitude	$t_{(17)} = 0.41, p = 0.69$
LRP latency	$t_{(17)} = 0.68, p = 0.51$
N2 amplitude	$t_{(17)} = 0.32, p = 0.75$
N2 latency	$t_{(17)} = 0.36, p = 0.73$
CRN amplitude	$t_{(17)} = 1.29, p = 0.22$
CRN latency	$t_{(17)} = 0.46, p = 0.65$
Contralateral	
P1 amplitude	$t_{(17)} = 0.66, p = 0.52$
P1 latency	$t_{(17)} = 0.21, p = 0.83$
N1 amplitude	$t_{(17)} = 1.44, p = 0.17$
N1 latency	$t_{(17)} = 0.57, p = 0.58$
Ipsilateral	
P1 amplitude	$t_{(17)} = 1.33, p = 0.20$
P1 latency	$t_{(17)} = 0.75, p = 0.46$
N1 amplitude	$t_{(17)} = 1.19, p = 0.25$
N1 latency	$t_{(17)} = 0.25, p = 0.80$

[a]All results from Experiment 2 replicate those obtained from Experiment 1, including the selective enhancement in the neural and behavioral indices of performance monitoring (A), the enhancement of neural and behavioral indices of learning (B, statistics based on learning rate parameter estimates), and the findings that numerous other neural and behavioral measures indexing other cognitive mechanisms were not significantly modulated by medial–frontal tDCS (C).

as the site of the reference electrode paired with the medial stimulation site (Experiment 1 vs 3; Fig. 10). This demonstrates that the medial cortex is the critical generator of the medial–frontal negativities and not a lateralized area in the path of the current flow (Gehring et al., 2012). Second, we replicated the tDCS effects on the ERN in a second experiment using an even simpler version of the task in which a different group of subjects made a simple detection response to targets unless countermanded by a stop signal (Experiment 4; Fig. 11). The stimulation conditions again changed only the medial–frontal ERN and not the ERP components indexing perceptual processing, response selection, or the waveforms recorded on correct trials. Thus, these follow-up experiments replicated and extended the behavioral and electrophysiological effects of medial–frontal tDCS we previously observed.

To visualize and model the brain areas affected by our tDCS manipulations, we computed a forward model of the current flow (De Lucia et al., 2007; Wagner et al., 2007b; Sadleir et al., 2010). Figure 10*A* shows the current flow during active tDCS based on our stimulation protocol and standard estimates of underlying anatomy and tissue properties. Electrical fields were modeled as extending through regions along the medial wall of frontal cortex, including SMA and ACC, but most likely affecting SMA and neighboring areas with higher intensity than ACC. To a lesser extent, right middle frontal and right superior temporal cortices

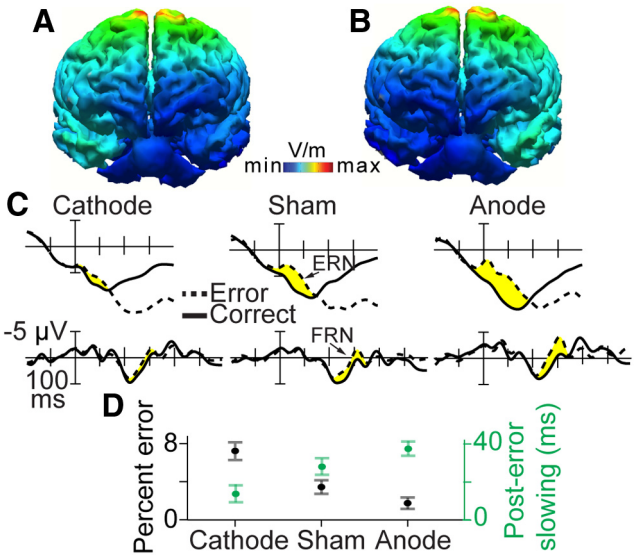

Figure 10. tDCS modeling and Experiment 3. The distributions of tDCS-modeled electrical fields shown projected through 3D reconstructions of the cortical surface. Forward models based on frontocentral midline anode and right cheek cathode electrode locations (***A***), and frontocentral midline anode and left cheek cathode electrode locations (***B***). Response-locked (top) and feedback stimulus-locked (bottom) grand average ERP waveforms from correct no-stop trials (black line) and errant no-stop trials (dashed line) shown at the central midline electrode (Cz) across sham, anodal, and cathodal conditions from Experiment 3 (***C***). Shaded yellow regions represent the latency window of the ERN (−50 to 150 ms relative to response onset) and FRN (200–400 ms relative to feedback onset). Mean percentage of stimulus-response mapping errors on no-stop trials and mean posterror slowing of RT after a failure to stop or a failure to map a stimulus to the correct response (***D***). Error bars indicate SEM. These ERPs were acquired after tDCS using the left cheek electrode location.

were implicated, but this appeared to be due to the location of the reference electrode. An additional model of tDCS current flow based on the left cheek reference electrode that we used in Experiment 3 also implicated SMA and ACC but spared the right-lateralized regions (Fig. 10*B*). To determine the involvement of these right-lateralized regions, we invited back the subjects who had participated in Experiment 1 to participate in another within-subjects 3-day tDCS and ERP experiment using a left cheek reference electrode (i.e., Experiment 3; 10 of 18 subjects returned for this experiment).

If right frontal and temporal lateral cortices were playing a critical role in the modulation of ERN and FRN by tDCS, then we should find that the tDCS effects are significantly reduced after tDCS using a left cheek reference. The ERP results from Experiment 3 are shown in Figure 10*C*. We found that the ERN and FRN components were clearly modulated by tDCS in the familiar cathodal < sham < anodal direction as reported in Experiment 1. To confirm these observations, we used nonparametric statistical tests (for details, see Materials and Methods) given the relatively small sample size ($N = 10$), but these results were also significant using parametric tests. We found a significant difference among the distributions of the three tDCS conditions for the ERN (−50 to 150 ms, $\chi_F^{2(2)} = 11.54, p < 0.01$) and FRN (200–400 ms, $\chi_F^{2(2)} = 8.60, p < 0.02$), based on pairwise Friedman's two-way ANOVAs by ranks. Specifically, we found that, relative to sham stimulation, anodal tDCS caused larger ERN (Wilcoxon signed-rank test, $z = 2.00, p < 0.05$) and FRN amplitudes ($z = 2.30, p < 0.03$), whereas cathodal tDCS caused smaller ERN ($z = 2.50, p < 0.02$) and FRN amplitudes ($z = 1.94, p < 0.04$). Indeed, after cathodal stimulation, there was no significant difference in the distributions among correct and error trials (i.e., ERN, $z = 1.73, p = 0.83$) or

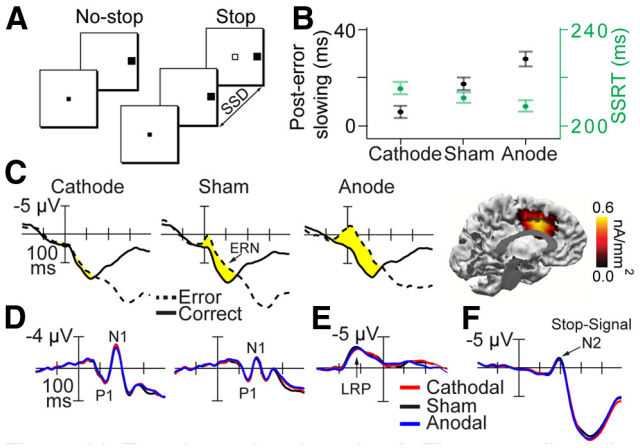

Figure 11. Experiment 4 and results. ***A***, The target discrimination task with stop signals requiring only a simple detection response. ***B***, Posterror slowing of RT using correction for nonstationarity and SSRT illustrated across sham, anodal, and cathodal conditions. Error bars indicate SEM. ***C***, Response-aligned grand average ERP waveforms from correct no-stop trials (solid line) and errant stop trials (dashed line) shown at the central midline electrode (Cz) across conditions. Shaded yellow regions represent the latency window of the ERN. The modeled distribution of ERN current density projected on a medial–sagittal slice of a 3D reconstruction of the cortical surface in the sham condition. Warmer colors represent greater current flow. ***D***, Target-aligned grand average correct no-stop ERP waves shown at lateral occipitotemporal sites (OL/OR), contralateral (left) and ipsilateral (right) with respect to target location for sham (green), cathodal (red), and anodal (blue) conditions. Labels show P1 and N1 components. ***E***, Response-locked grand average potential difference waves (contralateral − ipsilateral with respect to response hand) at central lateral electrodes (C3/C4) from correct no-stop trials across conditions as in ***D***. Arrow indicates the lateralized readiness potential. ***F***, Stop signal-locked grand average potentials on correct stop trials at the central midline electrode (Cz) across conditions as in ***D***. Arrow indicates the N2 component.

positive and negative feedback trials (i.e., FRN, $z = 0.65$, $p = 0.51$). In addition to these electrophysiological results, all behavioral results replicated the findings from Experiment 1, including significant bidirectional effects in stimulus-response mapping error rate (cathodal $z = 2.31$, $p < 0.03$; anodal $z = 2.52$, $p < 0.02$), posterror RT slowing (cathodal $z = 2.70$, $p < 0.01$; anodal $z = 2.55$, $p < 0.02$) (Fig. 10*D*; Table 1), and posterror accuracy (mean ± 95% within-subjects confidence interval, cathodal 91.4 ± 3.1%, $z = 2.42$, $p < 0.02$; anodal 99.3 ± 0.5%, $z = 3.20$, $p < 0.01$ relative to sham 96.3 ± 1.4%). We entered the ERP data into a mixed-model ANOVA with the data from the same subjects from Experiment 1 using the right cheek reference. This analysis yielded no significant interactions involving the reference site term (left vs right cheek, $p > 0.68$). These findings support the conclusion that stimulation of the medial–frontal structures, such as SMA and ACC, but not right middle frontal or superior temporal cortices, was critical in changing the medial–frontal negativities that we measured.

Experiment 1 demonstrates our causal manipulations of the medial–frontal negativities and behavior using a choice target discrimination task with stop signals and a learning manipulation. To determine the generality of our findings, we ran a different set of subjects ($N = 18$) through another 3 day tDCS and ERP experiment using a simple detection version of this discrimination task with no feedback stimuli or learning manipulation (i.e., Experiment 4; Fig. 11*A*). The findings from Experiment 4 replicated the fundamental results presented in Experiment 1 of a causal influence on the ERN, accompanied by changes in error-monitoring behavior (posterror slowing effects). This demonstrates that the effects of medial–frontal tDCS on the electrophysiological responses of the human brain and on behavior can be generalized to more basic laboratory tasks with fewer competing demands than in Experiment 1.

We found that performance related to adaptive control and behavioral monitoring in Experiment 4 was selectively influenced by the polarity of tDCS current flow. Posterror RT slowing was evident in the sham condition ($t_{(17)} = 3.87$, $p < 0.01$), reduced after cathodal stimulation ($t_{(17)} = 2.76$, $p < 0.02$), and increased after anodal stimulation ($t_{(17)} = 2.31$, $p < 0.03$) (Fig. 11*B*). However, a variety of other behavioral measures were uninfluenced by tDCS. There were no differences across tDCS conditions in the mean probability of responding on no-stop trials (mean ± 95% within-subjects confidence interval, cathodal 96.6 ± 1.8, sham 97.8 ± 2.1, anodal 97.1 ± 2; $p > 0.4$) or in the mean RT on no-stop trials (cathodal 518.5 ± 26 ms, sham 511.1 ± 29 ms, anodal 516.9 ± 23 ms; $p > 0.41$). Moreover, the speed and accuracy of response inhibition were not significantly modulated by tDCS. This was evidenced by measures of SSRT (Fig. 11*B*; $p > 0.11$) and inhibition errors on stop-signal trials (probability of any incorrect response on a stop trial, mean ± 95% within-subjects confidence interval, cathodal 54.1 ± 11, anodal 48.3 ± 7, sham 51.1 ± 4; $p > 0.25$). These results are consistent with those obtained in Experiment 1 using a choice discrimination task with stop signals and further reinforce the specificity of the tDCS effects on behavioral adjustments made after an error, but not other performance metrics.

Analyses of the ERN, CRN, P1, N1, LRP, and N2 from Experiment 4 replicated those results obtained in Experiment 1 and provide additional evidence that tDCS selectively influenced the ERN (Fig. 11*C*) and did not casually influence the amplitudes or latencies of these other ERP components. Specifically, a within-subjects ANOVA was computed with the factors of condition (anodal vs sham vs cathodal), trial type (correct vs error), and electrode site (Fz vs Cz vs Pz) on the amplitude of the waveforms during the ERN measurement window (−50 to 150 ms relative to response onset). A three-way interaction between condition × trial type × electrode site ($F_{(4,68)} = 5.19$, $p < 0.01$) was obtained and parsed with follow-up analyses for each of the three tDCS conditions. Significant effects of trial type and trial type × electrode site were observed for sham ($F_{(1,17)} = 40.87$, $p < 0.01$ and $F_{(2,34)} = 4.65$, $p < 0.02$, respectively) and anodal conditions ($F_{(1,17)} = 61.95$, $p < 0.01$ and $F_{(2,34)} = 38.04$, $p < 0.01$, respectively), but not for the cathodal condition ($F_{(1,17)} = 0.99$, $p = 0.33$ and $F_{(2,34)} = 1.39$, $p = 0.26$, respectively). As in our choice discrimination task, these results show that error trials elicited more negative potentials (i.e., the ERN) after sham and anodal tDCS and that larger ERNs followed anodal stimulation, whereas smaller ERNs followed cathodal stimulation (i.e., cathodal < sham < anodal).

In contrast to the effects we observed on the ERN during Experiment 4, we observed that none of the other ERP components significantly changed as a function of active tDCS (i.e., the CRN, P1, N1, LRP, and N2; Fig. 11*C–F*). This was evidenced by no main effects of condition on the amplitude of the CRN ($F_{(2,34)} = 0.22$, $p = 0.67$), P1 (contralateral $F_{(2,34)} = 0.04$, $p = 0.86$; ipsilateral $F_{(2,34)} = 0.10$, $p = 0.80$), N1 (contralateral $F_{(2,34)} = 1.85$, $p = 0.19$; ipsilateral $F_{(2,34)} = 0.77$, $p = 0.43$), LRP ($F_{(2,34)} = 0.72$, $p = 0.46$), or N2 ($F_{(2,34)} = 0.18$, $p = 0.84$). Additionally, there were no main effects of condition on the latency of the CRN ($F_{(2,34)} = 0.38$, $p = 0.67$), P1 (contralateral $F_{(2,34)} = 0.14$, $p = 0.74$; ipsilateral $F_{(2,34)} = 0.12$, $p = 0.83$), N1 (contralateral $F_{(2,34)} = 0.16$, $p = 0.71$; ipsilateral $F_{(2,34)} = 0.25$, $p = 0.64$), LRP ($F_{(2,34)} = 0.35$, $p = 0.57$), or N2 ($F_{(2,34)} = 0.18$, $p = 0.81$).

These results reinforce the conclusion that medial–frontal tDCS selectively modulated error-monitoring potentials and not other cognitive mechanisms indexed by the other ERP waveforms measured during the task.

Next, we computed a current-density model of the ERN component recorded during Experiment 4 (Fig. 11*C*). We found that the distribution of the current density model suggested plausible ERN neural generators within the dorsal bank of frontal cortex, including ACC and adjacent SMA (92% explained variance). The location of these reconstructed ERN current densities was consistent with our modeling results from Experiment 1 (Fig. 1*D*) as well as previous fMRI (Carter et al., 1998), ERP source modeling (Dehaene et al., 1994), and patient lesion studies (Swick and Turken, 2002). These results also show a tight correspondence with our modeled current flow of tDCS (Fig. 1*A*).

Experiments 1–4: error positivity

In addition to the ERN, research on error processing is focused on the positive-going waveform immediately after the ERN that is maximal over centroparietal cortex. The error positivity (or Pe) (Falkenstein et al., 1990; Gehring et al., 1993) is hypothesized to reflect error awareness and the affective response to the error (for review, see Falkenstein, 2004; Overbeek et al., 2005). Here, we asked whether our medial–frontal tDCS protocol influenced the amplitude of the Pe. An ANOVA with factors of stimulation condition (anodal vs cathodal vs sham), electrode site (Fz vs Cz vs Pz), and trial type (error vs correct) was computed on Pe amplitude (200–400 ms after response onset). For Experiment 1 using errant no-stop trials (Fig. 2*A*), we found a condition × electrode × trial type interaction ($F_{(4,68)} = 3.84, p < 0.02$). Follow-up ANOVAs for each midline electrode revealed that the largest change was at the Fz electrode as condition × trial type interactions were significant for both cathodal versus sham ($F_{(1,17)} = 5.00, p < 0.04$) and anodal versus sham comparisons ($F_{(1,17)} = 10.93, p < 0.01$). Similar results were obtained from Experiment 1 using errant stop trials (cathodal vs sham: $F_{(1,17)} = 4.60, p < 0.05$, anodal vs sham: $F_{(1,17)} = 5.10, p < 0.04$), Experiment 2 (anodal vs sham: $F_{(1,17)} = 4.24, p < 0.05$), Experiment 3 (cathodal vs sham: $F_{(1,9)} = 8.96, p < 0.02$, anodal vs sham: $F_{(1,9)} = 5.78, p < 0.04$), and Experiment 4 (cathodal vs sham: $F_{(1,17)} = 5.42, p < 0.03$, anodal vs sham: $F_{(1,17)} = 9.28, p < 0.01$).

These results demonstrate three findings: (1) errant responses elicited greater positive potential after the ERN (i.e., the Pe) in each stimulation condition across all experiments; (2) tDCS affected the distribution of the Pe, broadening its positivity over the front of the head after cathodal stimulation and narrowing its distribution across midline electrodes after anodal stimulation; and (3) the largest Pe values were observed after cathodal stimulation, whereas the smallest Pe values were observed after anodal stimulation. Thus, errors generated the expected late positivity in the sham condition, with the familiar distribution of effects shown across frontal, central, and parietal midline electrodes sites. Most important, cathodal stimulation in the same subjects boosted the Pe, whereas anodal stimulation over the same region reduced the amplitude of this component.

Discussion

Here we establish medial–frontal tDCS as a powerful causal tool for investigating the mechanisms that evaluate the output of cognitive processing and determine learning rate. There are a growing number of research domains and empirical phenomena being examined to determine the role played by medial–frontal cortex (e.g., Ridderinkhof et al., 2004; Amodio and Frith, 2006; Euston et al., 2012). Our results constrain models that cast medial–frontal cortex as a monitor of errors during information processing (Gehring et al., 2012) and as a high-level decision-making mechanism (Holroyd and Coles, 2002; Brown and Braver, 2005), generating training signals to drive learning as contingencies change (Walton et al., 2004; Behrens et al., 2007). Thus, our findings point to a possible reconciliation of diverse, but not mutually exclusive, theoretical perspectives on the functional significance of medial–frontal cortex.

We have shown that controlling the medial–frontal negativities with tDCS provides control over behavioral adaptations after error commission, which are taken as reflections of cognitive control processes. Models of compensatory behavior propose that such adjustments after high-interference events, including errors, occur from a decrease in baseline response activation or an increase in response threshold (e.g., Botvinick et al., 2001). Other proposals claim that posterror adjustments represent the behavioral manifestation of comparing outcomes with expectations (e.g., Holroyd et al., 2005) or reflect the continuation of a malfunctioning error-monitoring process (Gehring et al., 1993). Our study demonstrates the fertile ground for future work exploiting the causal control provided by tDCS to determine whether compensatory behavior is due to higher-order executive processes or engagement of a more reflexive, automatic phenomenon, such as the attentional orienting response to rare events (Notebaert et al., 2009).

We interpret the medial–frontal tDCS effects as due to the modulation of a performance-monitoring mechanism in the brain, serving as an online detector of information processing output and implementing adjustments needed to reinstate goal-directed behavior and support learning. However, an alternative explanation is that our stimulation changed the operation of response-selection mechanisms originating from pre-SMA. For example, cathodal tDCS might have induced noise in response-selection activity, thereby increasing error rates in our subjects. Our results from the LRP are inconsistent with this hypothesis. To further test this alternative explanation, we performed signal-to-noise ratio analyses based on each subject's waveforms in the 300 ms preceding response initiation (see Materials and Methods). We found that, across all four experiments, the variance of the ERPs did not change before response initiation between the stimulation conditions showing that the signal-to-noise ratios were similar (Experiment 1, $F_{(2,34)} = 1.48, p = 0.24$; Experiment 2, $F_{(1,17)} = 1.87, p = 0.21$; Experiment 3, $F_{(1,9)} = 1.21, p = 0.30$; Experiment 4: $F_{(2,34)} = 1.94, p = 0.17$). Thus, the operation of the cognitive mechanism of response selection does not appear to be the source of the changes in error-related behavior caused by tDCS. However, given the likelihood that the medial–frontal tDCS procedure activated pre-SMA, including its pathway to the subthalamic nucleus; and given previous work showing the involvement of this pathway in trial-to-trial behavior (Bogacz et al., 2010), the role of response-selection processes should not completely be ruled out.

Throughout we have interpreted the causal chain of events induced by tDCS as flowing from the electrophysiology of the brain to the behavior of the subject. This direction of causality is intuitive given our causal method of brain stimulation. It is also consistent with our findings that tDCS is influencing stop-trial electrophysiology, but not stop-trial behavioral errors (see above). However, our data cannot rule out the reverse order of causal events, from behavior to electrophysiology. It is possible that medial–frontal stimulation is directly affecting error-related behavior, changing error probability and leading to the observed

differences in ERN and FRN amplitude. For example, cathodal tDCS may be increasing error rates, thereby reducing the amplitude of the medial–frontal negativities because these components are sensitive to error likelihood. This interpretation is supported by previous studies showing that ERN amplitude is inversely correlated with error probability, such that infrequent errors produce larger ERNs (Gehring et al., 1993; Holroyd et al., 2005).

It is plausible that the feedback-related component we measured is not the FRN but rather the anterior N2. Like the FRN, the anterior N2 exhibits a frontocentral spatial distribution with a peak ~260 ms poststimulus onset and is thought to originate from the ACC (Holroyd, 2004; Foti et al., 2011). Unlike the FRN, which is sensitive to negative valence, the primary characteristic of the anterior N2 is its increase in negative amplitude as the eliciting stimulus occurs less frequently (Squires et al., 1976; Duncan-Johnson and Donchin, 1977). This is precisely the case in the sham condition of Experiments 1–3: as subjects proceed through the task, fewer errors are made and negative feedback occurs less often. The infrequency of task-relevant feedback events may be eliciting dips in dopamine activity, activating ACC and generating a larger N2 (Holroyd et al., 2008; Foti et al., 2011; Wessel et al., 2012). Under active tDCS conditions, the N2 amplitude is bidirectionally modulated, perhaps because of the manipulation of positive and negative reward prediction errors and their association with increased and decreased dopamine levels, respectively. Alternatively, the factual assumption in ERP research that the FRN and anterior N2 are two separate components indexing difference cognitive processes may be false. Instead, these components could be different manifestations of the same underlying phenomenon. Similarities in functional dependencies, morphology, amplitude, latency, polarity, and scalp distribution support this view (Holroyd, 2004).

Our Pe results dissociate two leading hypotheses about the functional relevance of the Pe component. One view holds that the Pe reflects conscious error monitoring as Pe amplitude has been shown to modulate with overt versus covert error commission (Vidal et al., 2000) and perceived versus unperceived saccadic errors (Nieuwenhuis et al., 2001). Our findings are inconsistent with this view because after cathodal stimulation the Pe was larger relative to the other conditions and subjects made more errors and exhibited weaker corrective behavior. Following this interpretation, greater error awareness indexed by the increased Pe amplitude should have reduced error rate and facilitated corrective behavior. An alternative proposal forwarded by Falkenstein et al. (2000) is that the Pe might index the subjective or emotional significance of the error. This explanation fits with our results. For example, cathodal stimulation might have increased the negative valence of the errors committed by the subjects. Evidence showing a relationship between medial–frontal cortex and affective processing provides further support for this interpretation (Bush et al., 2000).

Finally, our results suggest translational opportunities to improve cognitive control and learning in a variety of populations. Our study shows that anodal tDCS improves task accuracy and speeds learning, even in healthy adults who are already high functioning. This means that anodal tDCS of medial–frontal cortex has the potential to improve cognitive control and learning in a variety of task settings given that 20 min of noninvasive stimulation showed benefits for nearly 5 h. In addition to the potential to improve cognition during critical tasks performed by healthy individuals (e.g., pilots, soldiers, or students), the present methods may translate into clinical treatments in the near term. For example, it is known that patients with schizophrenia (Kopp and Rist, 1999; Frith et al., 2000; Alain et al., 2002; Bates et al., 2002; Mathalon et al., 2002; Morris et al., 2006), Alzheimer's disease (Mathalon et al., 2003), Huntington's disease (Beste et al., 2008), Parkinson's disease (Ito and Kitagawa, 2006; Stemmer et al., 2007), and attention deficit hyperactivity disorder (Schachar et al., 2004) all exhibit error-monitoring impairments. The present findings suggest that, with anodal stimulation, we could noninvasively treat such patients, potentially changing their performance to look more like healthy subjects.

References

Alain C, McNeely HE, He Y, Christensen BK, West R (2002) Neurophysiological evidence of error-monitoring deficits in patients with schizophrenia. Cereb Cortex 12:840–846. CrossRef Medline

Alexander WH, Brown JW (2011) Medial prefrontal cortex as an action-outcome predictor. Nat Neurosci 14:1338–1344. CrossRef Medline

Amodio DM, Frith CD (2006) Meeting of minds: the medial frontal cortex and social cognition. Nat Rev Neurosci 7:268–277. CrossRef Medline

Bates AT, Kiehl KA, Laurens KR, Liddle PF (2002) Error-related negativity and correct response negativity in schizophrenia. Clin Neurophysiol 113:1454–1463. CrossRef Medline

Batsikadze G, Moliadze V, Paulus W, Kuo MF, Nitsche MA (2013) Partially non-linear stimulation intensity-dependent effects of direct current stimulation on motor cortex excitability in humans. J Physiol 591:1987–2000. CrossRef Medline

Behrens TE, Woolrich MW, Walton ME, Rushworth MF (2007) Learning the value of information in an uncertain world. Nat Neurosci 10:1214–1221. CrossRef Medline

Berryhill ME, Wencil EB, Branch Coslett H, Olson IR (2010) A selective working memory impairment after transcranial direct current stimulation to the right parietal lobe. Neurosci Lett 479:312–316. CrossRef Medline

Beste C, Saft C, Konrad C, Andrich J, Habbel A, Schepers I, Jansen A, Pfleiderer B, Falkenstein M (2008) Levels of error processing in Huntington's disease: a combined study using event-related potentials and voxel-based morphometry. Hum Brain Mapp 29:121–130. CrossRef Medline

Bindman LJ, Lippold OC, Redfearn JW (1962) Long lasting changes in the level of the electrical activity of the cerebral cortex produced by polarizing currents. Nature 196:584–585. CrossRef Medline

Bogacz R, Wagenmakers EJ, Forstmann BU, Nieuwenhuis S (2009) The neural basis of the speed-accuracy tradeoff. Trends Neurosci 33:10–16. CrossRef Medline

Botvinick MM, Braver TS, Barch DM, Carter CS, Cohen JD (2001) Conflict monitoring and cognitive control. Psychol Rev 108:624–652. CrossRef Medline

Brewer N, Smith GA (1989) Developmental changes in processing speed: influence of speed–accuracy regulation. J Exp Psychol 118:298–310. CrossRef

Brown JW, Braver TS (2005) Learned predictions of error likelihood in the anterior cingulate cortex. Science 307:1118–1121. CrossRef Medline

Bush G, Luu P, Posner MI (2000) Cognitive and emotional influences in anterior cingulate cortex. Trends Cogn Sci 4:215–222. CrossRef Medline

Carter CS, Braver TS, Barch DM, Botvinick MM, Noll D, Cohen JD (1998) Anterior cingulate cortex, error detection, and the online monitoring of performance. Science 280:747–749. CrossRef Medline

Clayson PE, Baldwin SA, Larson MJ (2013) How does noise affect amplitude and latency measurement of event-related potentials (ERPs)? A methodological critique and simulation study. Psychophysiology 50:174–186. CrossRef Medline

Cohen JD, Botvinick M, Carter CS (2000) Anterior cingulate and prefrontal cortex: who's in control? Nat Neurosci 3:421–423. CrossRef Medline

Dale AM, Sereno MI (1993) Improved localization of cortical activity by combining EEG and MEG with MRI cortical surface reconstruction: a linear approach. J Cogn Neurosci 5:162–176. CrossRef Medline

Dehaene S, Posner MI, Tucker DM (1994) Localization of a neural system for error detection and compensation. Psychol Sci 5:303–305. CrossRef

De Lucia M, Parker GJ, Embleton K, Newton JM, Walsh V (2007) Diffusion tensor MRI-based estimation of the influence of brain tissue anisotropy on the effects of transcranial magnetic stimulation. Neuroimage 36:1159–1170. CrossRef Medline

Duncan-Johnson CC, Donchin E (1977) On quantifying surprise: the variation of event-related potentials with subjective probability. Psychophysiology 14:456–467. CrossRef Medline

Eason R, Harter M, White C (1969) Effects of attention and arousal on visually evoked cortical potentials and reaction time in man. Physiol Behav 4:283–289. CrossRef

Euston DR, Gruber AJ, McNaughton BL (2012) The role of medial prefrontal cortex in memory and decision making. Neuron 76:1057–1070. CrossRef Medline

Falkenstein M (2004) ERP correlates of erroneous performance. In: Errors, conflicts, and the brain: current opinions on performance monitoring (Ullsperger M, Falkenstein M, eds), pp 5–14. Leipzig, Germany: Max Planck Institute of Cognitive Neuroscience.

Falkenstein M, Hohnsbein J, Blanke L (1990) Effects of errors in choice reaction tasks on the ERP under focused and divided attention. In: Psychophysiological brain research (Brunia CH, Gaillard AW, Kok A, eds), pp 192–195. Tilburg, The Netherlands: Tilburg UP.

Falkenstein M, Hoormann J, Christ S, Hohnsbein J (2000) ERP components on reaction errors and their functional significance: a tutorial. Biol Psychol 51:87–107. CrossRef Medline

Foti D, Weinberg A, Dien J, Hajcak G (2011) Event-related potential activity in the basal ganglia differentiates rewards from nonrewards: temporospatial principal components analysis and source localization of the feedback negativity. Hum Brain Mapp 32:2207–2216. CrossRef Medline

Frith CD, Blakemore S, Wolpert DM (2000) Explaining the symptoms of schizophrenia: abnormalities in the awareness of action. Brain Res Rev 31:357–363. CrossRef Medline

Gehring WJ, Willoughby AR (2002) The medial frontal cortex and the rapid processing of monetary gains and losses. Science 295:2279–2282. CrossRef Medline

Gehring WJ, Gross B, Coles MGH, Meyer DE, Donchin E (1993) A neural system for error detection and compensation. Psychol Sci 4:385–390. CrossRef

Gehring WJ, Liu Y, Orr JM, Carp J (2012) The error-related negativity (ERN/Ne). In: Oxford handbook of event-related potential components (Luck SJ, Kappenman E, eds), pp 231–291. New York: Oxford UP.

Godlove DC, Emeric EE, Segovis CM, Young MS, Schall JD, Woodman GF (2011) Event-related potentials elicited by errors during the stop-signal task: I. Macaque monkeys. J Neurosci 31:15640–15649. CrossRef Medline

Hanes DP, Patterson WF 2nd, Schall JD (1998) Role of frontal eye fields in countermanding saccades: visual, movement, and fixation activity. J Neurophysiol 79:817–834. Medline

Holroyd CB (2004) A note on the oddball N200 and the feedback ERN. In: Errors, conflicts, and the brain: current opinions on performance monitoring (Ullsperger M, Falkenstein M, eds), pp 211–218. Leipzig, Germany: Max Planck Institute of Cognitive Neuroscience.

Holroyd CB, Coles MG (2002) The neural basis of human error processing: reinforcement learning, dopamine, and the error-related negativity. Psychol Rev 109:679–709. CrossRef Medline

Holroyd CB, Yeung N, Coles MG, Cohen JD (2005) A mechanism for error detection in speeded response time tasks. J Exp Psychol 134:163–191. CrossRef Medline

Holroyd CB, Pakzad-Vaezi KL, Krigolson OE (2008) The feedback correct-related positivity: sensitivity of the event-related brain potential to unexpected positive feedback. Psychophysiology 45:688–697. CrossRef Medline

Hsu TY, Tseng LY, Yu JX, Kuo WJ, Hung DL, Tzeng OJ, Walsh V, Muggleton NG, Juan CH (2011) Modulating inhibitory control with direct current stimulation of the superior medial frontal cortex. Neuroimage 56:2249–2257. CrossRef Medline

Ito J, Kitagawa J (2006) Performance monitoring and error processing during a lexical decision task in patients with Parkinson's disease. J Geriatr Psychiatry Neurol 19:46–54. CrossRef Medline

Ito S, Stuphorn V, Brown JW, Schall JD (2003) Performance monitoring by the anterior cingulate cortex during saccade countermanding. Science 302:120–122. CrossRef Medline

Jennings JR, Wood CC (1976) The e-adjustment procedure for repeated-measures analyses of variance. Psychophysiology 13:277–278. CrossRef Medline

Kiesel A, Miller J, Jolicoeur P, Brisson B (2008) Measurement of ERP latency differences: a comparison of single-participant and jackknife-based scoring methods. Psychophysiology 45:250–274. CrossRef Medline

Kopp B, Rist F (1999) An event-related brain potential substrate of disturbed response monitoring in paranoid schizophrenic patients. J Abnorm Psychol 108:337–346. CrossRef Medline

Laming D (1968) Information theory of choice reaction times. London: Academic.

Logan GD, Cowan WB, Davis KA (1984) On the ability to inhibit responses in simple and choice reaction time tasks: a model and a method. J Exp Psychol Hum Percept Perform 10:276–291. Medline

Luck SJ (2005) An introduction to the event-related potential technique. Cambridge, MA: Massachusetts Institute of Technology.

Luck SJ, Hillyard SA (1990) Electrophysiological evidence for parallel and serial processing during visual search. Percept Psychophys 48:603–617. CrossRef Medline

Mathalon DH, Fedor M, Faustman WO, Gray M, Askari N, Ford JM (2002) Response-monitoring dysfunction in schizophrenia: an event-related brain potential study. J Abnorm Psychol 111:22–41. CrossRef Medline

Mathalon DH, Bennett A, Askari N, Gray EM, Rosenbloom MJ, Ford JM (2003) Response-monitoring dysfunction in aging and Alzheimer's disease: an event-related potential study. Neurobiol Aging 24:675–685. CrossRef Medline

Miller J, Patterson T, Ulrich R (1998) Jackknife-based method for measuring LRP onset latency differences. Psychophysiology 35:99–115. CrossRef Medline

Miltner WH, Braun CH, Coles MG (1997) Event-related brain potentials following incorrect feedback in a time-estimation task: evidence for a "generic" neural system for error detection. J Cogn Neurosci 9:788–798. CrossRef Medline

Monte-Silva K, Kuo MF, Hessenthaler S, Fresnoza S, Liebetanz D, Paulus W, Nitsche MA (2013) Induction of late LTP-like plasticity in the human motor cortex by repeated non-invasive brain stimulation. Brain Stimul 6:424–432. CrossRef Medline

Morris SE, Yee CM, Nuechterlein KH (2006) Electrophysiological analysis of error monitoring in schizophrenia. J Abnorm Psychol 115:239–250. CrossRef Medline

Nelson MJ, Boucher L, Logan GD, Palmeri TJ, Schall JD (2010) Nonindependent and nonstationary response times in stopping and stepping saccade tasks. Atten Percept Psychophys 72:1913–1929. CrossRef Medline

Nieuwenhuis S, Ridderinkhof KR, Blom J, Band GP, Kok A (2001) Error-related brain potentials are differentially related to awareness of response errors: evidence for an antisaccade task. Psychophysiology 38:752–760. CrossRef Medline

Nitsche MA, Paulus W (2000) Excitability changes induced in the human motor cortex by weak transcranial direct current stimulation. J Physiol 527:633–639. CrossRef Medline

Nitsche MA, Paulus W (2001) Sustained excitability elevations induced by transcranial DC motor cortex stimulation in humans. Neurology 57:1899–1901. CrossRef Medline

Nitsche MA, Liebetanz D, Antal A, Lang N, Tergau F, Paulus W (2003a) Modulation of cortical excitability by weak direct current stimulation: technical, safety and functional aspects. Suppl Clin Neurophysiol 56:255–276. CrossRef Medline

Nitsche MA, Liebetanz D, Lang N, Antal A, Tergau F, Paulus W (2003b) Safety criteria for transcranial direct current stimulation (tDCS) in humans. Clin Neurophysiol 114:2220–2222; author reply 2222–2223 CrossRef Medline

Nitsche MA, Nitsche MS, Klein CC, Tergau F, Rothwell JC, Paulus W (2003c) Level of action of cathodal DC polarisation induced inhibition of the human motor cortex. Clin Neurophysiol 114:600–604. CrossRef Medline

Notebaert W, Houtman F, Opstal FV, Gevers W, Fias W, Verguts T (2009) Post-error slowing: an orienting account. Cognition 111:275–279. CrossRef Medline

Nunez PL, Srinivasan R (2006) Electric fields of the brain: the neurophysics of EEG, Ed 2. Oxford: Oxford UP.

Overbeek TJM, Nieuwenhuis S, Ridderinkhof KR (2005) Dissociable components of error processing: on the functional significance of the Pe vis-a-vis the ERN/Ne. J Psychophysiol 19:319–329. CrossRef

Pascual-Marqui RD (2002) Standardized low-resolution brain electromagnetic tomography (sLORETA): technical details. Methods Find Exp Clin Pharmacol 24:5–12. Medline

Pliszka SR, Liotti M, Woldorff MG (2000) Inhibitory control in children with attention-deficit/hyperactivity disorder: event-related potentials

identify the processing component and timing of an impaired right-frontal response-inhibition mechanism. Biol Psychiatry 48:238–246. CrossRef Medline

Rabbitt P, Rodgers B (1977) What does a man do after he makes an error? An analysis of response programming. Q J Exp Psychol 29:727–743. CrossRef

Rabbitt PM (1966) Error correction time without external error signals. Nature 212:438. CrossRef Medline

Reinhart RM, Carlisle NB, Kang MS, Woodman GF (2012) Event-related potentials elicited by errors during the stop-signal task: II. Human effector specific error responses. J Neurophysiol 107:2794–2807. CrossRef Medline

Ridderinkhof KR, Ullsperger M, Crone EA, Nieuwenhuis S (2004) The role of the medial frontal cortex in cognitive control. Science 306:443–447. CrossRef Medline

Rollnik JD, Schröder C, Rodríguez-Fornells A, Kurzbuch AR, Däuper J, Möller J, Münte TF (2004) Functional lesions and human action monitoring: combining repetitive transcranial magnetic stimulation and event-related brain potentials. Clin Neurophysiol 115:145–153. CrossRef Medline

Sadleir RJ, Vannorsdall TD, Schretlen DJ, Gordon B (2010) Transcranial direct current stimulation (tDCS) in a realistic head model. Neuroimage 51:1310–1318. CrossRef Medline

Schachar RJ, Chen S, Logan GD, Ornstein TJ, Crosbie J, Ickowicz A, Pakulak A (2004) Evidence for an error monitoring deficit in attention deficit hyperactivity disorder. J Abnormal Child Psychol 32:285–293. CrossRef Medline

Schmajuk M, Liotti M, Busse L, Woldorff MG (2006) Electrophysiological activity underlying inhibitory control processes in normal adults. Neuropsychologia 44:384–395. CrossRef Medline

Schroder HS, Infantolino ZP (2013) Distinguishing between types of errors and adjustments. J Neurosci 33:1835–1837.

Sheth SA, Mian MK, Patel SR, Asaad WF, Williams ZM, Dougherty DD, Bush G, Eskandar EN (2012) Human dorsal anterior cingulate cortex neurons mediate ongoing behavioural adaptation. Nature 488:218–221. CrossRef Medline

Smulders FTY, Miller JO (2012) The lateralized readiness potential. In: Oxford handbook of event-related potential components (Luck SJ, Kappenman E, eds), pp 209–229. New York: Oxford UP.

Squires KC, Wickens C, Squires NK, Donchin E (1976) The effect of stimulus sequence on the waveform of the cortical event-related potential. Science 193:1142–1146. CrossRef Medline

Stemmer B, Segalowitz SJ, Dywan J, Panisset M, Melmed C (2007) The error negativity in nonmedicated and medicated patients with Parkinson's disease. Clin Neurophysiol 118:1223–1229. CrossRef Medline

Swick D, Turken AU (2002) Dissociation between conflict detection and error monitoring in the human anterior cingulate cortex. Proc Natl Acad Sci U S A 99:16354–16359. CrossRef Medline

Tseng P, Hsu TY, Chang CF, Tzeng OJ, Hung DL, Muggleton NG, Walsh V, Liang WK, Cheng SK, Juan CH (2012) Unleashing potential: transcranial direct current stimulation over the right posterior parietal cortex improves change detection in low-performing individuals. J Neurosci 32:10554–10561. CrossRef Medline

Utz KS, Dimova V, Oppenländer K, Kerkhoff G (2010) Electrified minds: transcranial direct current stimulation (tDCS) and galvanic vestibular stimulation (GVS) as methods of non-invasive brain stimulation in neuropsychology: a review of current data and future implications. Neuropsychologia 48:2789–2810. CrossRef Medline

van Driel J, Ridderinkhof KR, Cohen MX (2012) Not all errors are alike: theta and alpha EEG dynamics relate to differences in error-processing dynamics. J Neurosci 32:16795–16806. CrossRef Medline

Van Voorhis ST, Hillyard SA (1977) Visual evoked potentials and selective attention to points in space. Percept Psychophys 22:54–62. CrossRef

Verbruggen F, Logan GD (2008) Long-term aftereffects of response inhibition: memory retrieval task goals and cognitive control. J Exp Psychol 34:1229–1235. CrossRef Medline

Verbruggen F, Logan GD, Liefooghe B, Vandierendonck A (2008) Short-term aftereffects of response inhibition: repetition priming or between-trial control adjustments? J Exp Psychol 34:413–426. CrossRef Medline

Vidal F, Hasbroucq T, Grapperon J, Bonnet M (2000) Is the 'error negativity' specific to errors? Biol Psychology 51:109–128. CrossRef Medline

Wagner M, Fuchs M, Kastner J (2007a) SWARM: sLORETA-weighted accurate minimum norm inverse solutions. International Congress Series 1300:185–188. CrossRef

Wagner T, Fregni F, Fecteau S, Grodzinsky A, Zahn M, Pascual-Leone A (2007b) Transcranial direct current stimulation: a computer-based human model study. Neuroimage 35:1113–1124. CrossRef Medline

Walton ME, Devlin JT, Rushworth MF (2004) Interactions between decision making and performance monitoring within prefrontal cortex. Nat Neurosci 7:1259–1265. CrossRef Medline

Wessel JR, Danielmeier C, Morton JB, Ullsperger M (2012) Surprise and error: common neuronal architecture for the processing of errors and novelty. J Neurosci 32:7528–7537. CrossRef Medline

Woodman GF (2010) A brief introduction to the use of event-related potentials (ERPs) in studies of perception and attention. Atten Percept Psychophys 72:2031–2046. CrossRef Medline

Woodman GF, Luck SJ (2003) Serial deployment of attention during visual search. J Exp Psychol 29:121–138. CrossRef Medline

Zhua L, Mathewson KE, Hsu M (2012) Dissociable neural representations of reinforcement and belief prediction errors underlie strategic learning. Proc Natl Acad Sci U S A 109:1419–1424. CrossRef Medline